Internal Report
DESY M 98-03
May 1998

Studies of the Behaviour of Proton Spin Motion in HERA-p at High Energies

Part II. Acceleration of Polarized Protons in HERA

V.V. Balandin, N.I. Golubeva

Institute for Nuclear Research of RAS, Moscow, Russia

D.P. Barber

Deutsches Elektronen-Synchrotron DESY, Hamburg, Germany

DESY behält sich alle Rechte für den Fall der Schutzrechtserteilung und für die wirtschaftliche Verwertung der in diesem Bericht enthaltenen Informationen vor.

DESY reserves all rights for commercial use of information included in this report, especially in case of filing application for or grant of patents.

"Die Verantwortung für den Inhalt dieses
Internen Berichtes liegt ausschließlich beim Verfasser"

Studies of the Behaviour of Proton Spin Motion in HERA-p at High Energies

Part II. Acceleration of Polarized Protons in HERA

V.V, Balandin *, D.P. Barber † and N.I. Golubeva *

* *Institute for Nuclear Research of RAS,*
60th October Anniversary Pr., 7a, Moscow 117 312, Russia
† *Deutsches Elektronen-Synchrotron DESY, Hamburg*

Abstract

This report is the logical continuation of the paper [1]. It is a working report where we present several more or less consistent series of results which in our opinion could be interesting for other researchers.

As in [1] we again do not try to explain "why"?, but simply show the numerical results obtained for the real structure of the real accelerator.

1 Introduction

The idea to try to obtain a polarized proton beam in HERA at the top energy emerged in DESY sometime in 1994 after the achievement of longitudinal spin polarization in the HERA electron ring [2] in May 1994, and since the first paper discussing this problem was published [3] extensive studies have been made by several groups of people whose names can be found in the report [4].

The first key problem for spin motion in the HERA proton ring was that there are stretches of interleaved horizontal and vertical bends on each side of the East, South and North interaction points; the HERA proton ring is not planar. However, as pointed out for the first time in [5], owing to the mirror symmetry of these sections with respect to the interaction points, the effect of the vertical bends on the spin motion can be compensated just by inserting Siberian Snakes. This result was published in [1] where it was also shown that without considering how to obtain a polarized proton beam at the final energy, the polarization may be conserved even with one full snake in the ring if we do not take into account misalignments of electromagnetic elements in the accelerating structure.

In our opinion, the current problems which we have to solve and which require reliable solutions can be separated into the following three groups

- Injection of the polarized beam at $40\,GeV$
- Acceleration form $40\,GeV$ to $820\,GeV$
- Providing long lifetime of the polarized beam at $820\,GeV$

In this working report we present several more or less consistent series of figures which were obtained by numerical simulations. This figures are mainly connected with item two in the above list.

2 The Models of the HERA-p Lattice Used

For the investigations presented in this report we use the 1996 HERA-p luminosity optic. The South and North interaction sections have the same optic in the regions where the vertical bends are interleaved with horizontal bends. To increase the possible number of symmetries we have also studied the nonflat optic of HERA-p where the vertical bends are switched off in

the East. In order to compare the results obtained with the results of other projects and also for comparison of the behaviour of the spin vector in flat and nonflat rings we have also studied a flat test model obtained by removing the vertical bends in all interaction sections.

The betatron tunes and the synchrotron tune at the energy $E = 820GeV$ are shown in the following table.

Ring Model	Tunes		
	Q_x	Q_y	Q_z
Luminosity optic	31.28032	32.2723	0.00064
Vertical bends in the East are switched off	31.28006	32.2723	0.00064
Flat test model	31.27898	32.2723	0.00064

The vertical betatron tune Q_y and the synchrotron tune Q_z are model independent. The horizontal tune Q_x has slight model dependence. Thus all models are very close to each other with respect to betatron oscillations. Comparison of the linear optical functions of all rings gives approximately the same level of similarity as in [1] for the 1995 HERA-p luminosity optic, so that we shall not plot them here.

3 Useful Notations

To describe the six-dimensional orbital motion we shall use the variables

$$x, \quad P_x, \quad y, \quad P_y, \quad z, \quad P_z$$

where x and y are the transverse deviations of particle position from the design orbit with the property that for the flat parts of the ring they become horizontal and vertical deviations respectively. P_x and P_y are the corresponding transverse momenta normalized to the value of the design kinetic momentum π_0, z describes the longitudinal separation of the particle

from the reference particle and the quantity P_z is proportional to their fractional energy deviation:

$$P_z = \frac{\Delta E}{\beta_0^2 E_0}$$

The spin motion is described by the Thomas-BMT equations [6, 7] for the classical spin vector $\vec{s} = (s_x, s_y, s_z)$ written using the length along the design orbit τ as the independent variable

$$\frac{d\vec{s}}{d\tau} = \vec{\Omega}(\tau, x, P_x, y, P_y, z, P_z, \gamma_0) \times \vec{s} \tag{1}$$

Here γ_0 is Lorentz factor of the reference particle.

By substituting the 6-dimensional closed orbit of betatron and synchrotron oscillations[1]

$$\tilde{x}(\tau, \gamma_0), \ \tilde{P}_x(\tau, \gamma_0), \ \tilde{y}(\tau, \gamma_0), \ \tilde{P}_y(\tau, \gamma_0), \ \tilde{z}(\tau, \gamma_0), \ \tilde{P}_z(\tau, \gamma_0)$$

into (1) we obtain the system

$$\frac{d\vec{s}}{d\tau} = \vec{\Omega}_0(\tau, \gamma_0) \times \vec{s} \tag{2}$$

which describes spin motion in zeroth approximation with respect to orbital oscillations. If the one turn revolution matrix of the system (2) is not equal to the identity matrix then these equations have a unique periodic solution $\vec{n}_0(\tau, \gamma_0)$ satisfying the condition $|\vec{n}_0(\tau, \gamma_0)| \equiv 1$.

4 FORGET-ME-NOT, a Computer Code for the Study of Polarized Beam Dynamics

All numerical results presented in this paper were obtained with the help of the computer code **FORGET-ME-NOT** (this code was presented for the first time in 1992 under the name "VasiLIE" [8]). This computer code has been written for the study of unpolarized and polarized beam dynamics and some details of its possibilities and examples of applications are listed below.

[1] In the absence of misalignments this closed orbit is assumed to coincide with the solution for the reference particle.

4.1 Some Important Options

- Calculation of the strengths of imperfection spin resonances and first order intrinsic spin resonances for betatron oscillations with the help of the averaging method (the numerical scheme is based on the definitions which can be found in [9, 10, 1]). This method allows us to calculate not only strengths and locations of first order intrinsic resonances for rings with partial snakes, solenoids and strongly tilted dipole magnets (for example, vertical bending magnets in the HERA-p ring) but also first order spin tune shift (including the part which is often called spin chromaticity). In the cases when synchrotron oscillations are not taken into account and the optical structure of the accelerator allows the DEPOL program [11] to be used, the computer code FORGET-ME-NOT gives the same results.

- Calculation and analysis of nonlinear effects with the help of truncated Taylor maps. FORGET-ME-NOT allows us to calculate the one-turn Taylor map for six-dimensional orbital motion plus, if necessary, three-dimensional spin motion up to arbitrary order in the betatron and synchrotron oscillation amplitudes. This map can be used for tracking studies or it can be the starting point of a normal form analysis for determining the invariant functions of the orbit motion, equilibrium polarization direction and dependence of orbit and spin tunes on the invariants of orbit motion (spread of orbit and spin tunes). Note that FORGET-ME-NOT was the first computer code to provide these possibilities for spin motion and all our tools for analysis of spin maps are based on the new algorithms derived by its authors [12, 13, 14, 15].

- Tracking of particles with spin in accelerators and storage rings preserving symplecticity with respect to the 6-D orbit motion and orthogonality with respect to the 3-D spin motion. The numerical schemes used in FORGET-ME-NOT are based on canonical methods for the integration of spin-orbit equations of motion (in analogy to the symplectic numerical methods for the orbital dynamics) introduced in the field of accelerator physics for the first time by its authors [8, 9, 12].

- Among other available options, we would like to mention possibilities to obtain linear optical functions for spin and orbit motion, to calculate periodic solutions (closed orbits) for spin and orbit motion in the

presence of misalignments and to use time dependent electromagnetic elements (pulsed dipoles and quadrupoles, RF dipoles, spin flippers) during tracking calculations.

- Currently under construction and soon to be available for both orbital and spin motion will be possibilities to take into account stochastic fluctuations of values of magnetic and electric fields, stochastic vibrations of optical elements in accelerator structures, influence of beam-beam and space charge effects (note that space charge simulations are available now in FORGET-ME-NOT for transverse orbital dynamics only).

4.2 Examples of Applications

- The investigation of schemes for preserving the polarization in the TRIUMF KAON Booster [9, 16]. This involved the simulation of a whole acceleration cycle for a polarized proton beam, including misalignments of optical elements, closed orbit correction, partial Siberian snakes (two solenoids each 0.5 meter long with a 0.5 T field placed in a straight section) and switching on and off four pulsed quadrupoles at chosen moments.

- The influence of the space charge effect on slow resonance beam extraction from the Booster of the Moscow KAON Factory [17, 18]. Here it was important to understand the negative effect of space charge near a third-integer resonance and to develop compensation schemes using octupoles (and higher order multipoles).

- The study of the possibility to accelerate the polarized proton beam in the Nuclotron ring in Dubna [19]. Here we have an example of a low energy ring (maximum energy of the protons 10-12 GeV) with only four intrinsic resonances in the acceleration region which, nevertheless, are so strong that it is impossible to cross them with the help of betatron tune jumps without correcting their strengths (or without some other changes in the optical structure of the accelerator).

- The investigation of spin motion up to high energies in the HERA proton ring [1]. This topic is the subject of the present paper so that we shall not put any additional comments here.

5 More Details about the Numerical Calculations Presented in this Paper

To track particles with spin, FORGET-ME-NOT allows us to choose not only the number of numerical integration steps per element but also the complexity of the model of the motion (including for example, if necessary, fringe field effects in thin lens integral approximation).

All available possibilities were carefully investigated and, making a compromise between high speed for the calculations and the precision of the model, we decided to use a Hamiltonian which contains all terms up to order 3 with respect to coupled synchro-betatron oscillations for the orbital dynamics and to keep all terms up to order 2 with respect to the orbital variables in the equations of spin motion for all elements in the accelerator structure. Besides that, of course, we use terms of high order for octupoles and other multipoles. The number of integration steps per element is chosen to be the same as in [1].

To give an experienced reader a better impression about the exact model of motion used for the calculations presented in this paper, we print below the orbital Hamiltonian and the components of the vector $\vec{\Omega}$ entering the corresponding Thomas-BMT equations of spin motion (1) for the body of a horizontal combined function magnet in the arc of the HERA-p ring.

$$H_{orbt} = \frac{1}{2}(1 - P_z)\left(P_x^2 + P_y^2 + \frac{1}{\gamma_0^2}P_z^2\right) +$$

$$+ \left((k_0 - h) - h\left(1 - \frac{1}{2\gamma_0^2}P_z\right)P_z\right)x + (k_1 + hk_0)\frac{x^2}{2} - k_1\frac{y^2}{2} +$$

$$+ h\,k_1\frac{2x^3 - 3xy^2}{6} + \frac{h}{2}x\left(P_x^2 + P_y^2\right) + k_2\frac{x^3 - 3xy^2}{6}$$

$$\Omega_x = -k_0(1 - \gamma_0)\,G\,P_x\,P_y - (h\,k_1 + k_2)(1 + \gamma_0\,G)\,x\,y -$$

$$- k_1\left(1 + \gamma_0\,G - \left(1 + \frac{G}{\gamma_0}\right)P_z\right)y$$

$$\Omega_y \;=\; h \;-\; k_0\,(1+\gamma_0\,G) \;+\; k_0\,\left(1 \;+\; \frac{G}{\gamma_0}\right)\,(1-P_z)\;P_z \;-$$

$$-\,(k_1 \;+\; h\,k_0)\left(1 \;+\; \gamma_0\,G \;-\; \left(1 \;+\; \frac{G}{\gamma_0}\right)\,P_z\right)\,x \;-\; k_0\,(1-\gamma_0)\,G\,P_y^2 \;-$$

$$-\,\frac{1\;+\;\gamma_0\,G}{2}\,\left(k_0\,\left(P_x^2 \;+\; P_y^2 \;+\; \frac{1}{\gamma_0^2}P_z^2\right) \;+\; (2h\,k_1 \;+\; k_2)\,x^2 \;-\; (h\,k_1 \;+\; k_2)\,y^2\right)$$

$$\Omega_z \;=\; -(1 \;-\; \gamma_0)\,G\,\left(k_0\,\left(1 \;+\; h\,x \;+\; \frac{1-\gamma_0}{\gamma_0}\,P_z\right)\,P_y \;+\; k_1\,(x\,P_y \;+\; y\,P_x)\right)$$

Here γ_0 is the Lorentz factor of the reference particle, $G = (g-2)/2$ quantifies the anomalous spin g factor, h is the horizontal curvature of the reference orbit and k_0, k_1, k_2 are strengths of dipole, quadrupole and sextupole components respectively.

6 Numerical Modelling of the Acceleration Cycle

We now begin to discuss the numerical simulation of acceleration.

The ramp at HERA-p is provided by two different RF systems and takes approximately twenty minutes. The acceleration rate changes with energy approximately in accordance with the following table

Full Energy (GeV)	**Acceleration Rate (KeV/Turn)**
40	≈ 12.0
50	≈ 14.6
60	≈ 15.4
70	≈ 17.0
90	≈ 17.0
180	≈ 17.0
200	≈ 20.0
280	≈ 21.0
300	≈ 24.0
820	≈ 40.0

In our numerical simulations:

- We shall use a ramping speed which is the result of linear interpolation using the above table. Acceleration will be provided by setting the voltages and phases of RF cavities correspondingly.
- We shall not take into account additional nonlinearities at low energies due to persistent currents in superconducting magnets.
- We shall not change the transverse optic from flat bottom to flat top and for the whole acceleration cycle we use the transverse luminosity optic.

6.1 The Snake Configuration and the Ring Model Chosen for Numerical Simulations

By introducing one full longitudinal snake at the West and one full radial snake at the North, South and East interaction points (IP's) respectively we obtain a spin tune of $1/2$ in zeroth approximation with respect to orbital oscillations and a vertical $\vec{n}_0$ at the East IP at all energies[2]. But the behaviour of the vector $\vec{n}_0(\tau, \gamma_0)$ along the ring in the nonplanar HERA-p is not simple even in the presence of snakes: this vector is usually not vertical along the ring and depends strongly on the energy. If we require that $\vec{n}_0(\tau, \gamma_0)$ is vertical at all IP's at all energies we need some additional changes in the optic. One way to proceed is proposed in [4]. A full radial snake is inserted at the midpoint of each section containing two opposite polarity vertical bends and two identical horizontal bends, so that the whole section is equivalent to a full radial snake. These snakes are called flattening snakes (FS). So in the general case of the nonplanar HERA we have to use 6 additional full radial snakes and in the case of a geometry without vertical bends in the East section - just 4 full radial snakes.

Taking into account the points formulated above, for the first tracking studies of the acceleration cycle in HERA we chose the nonplanar ring model without vertical bends in the East equipped with the four basic snakes already mentioned and four additional flattening snakes.

[2]Note that this snake configuration was already considered in [1] for the top energy of 820 GeV and demonstrated quite stable behaviour of the polarization in the storage mode.

Naturally, it would not be possible to place snakes right at the IP's in practice, but there are free spaces at 0°, 85.54°, 180.04° and 273.53° (measuring clockwise from the East IP) where it is possible to put snakes, as was done in our previous numerical simulations [3].

Note that in this report we always work with idealized snakes which influence all the spins in the same way independently of particle position in phase space and which do not influence the orbit.

6.2 Initial Conditions

We have taken the initial energy to be 40 GeV. The transverse invariant emittances were chosen to be $\varepsilon_x = \varepsilon_y = 4 \cdot 10^{-6} mrad$. This value corresponds to the 1σ beam size. The longitudinal emittance is taken to be $\varepsilon_z = 0.021 eV \cdot s$. This corresponds to a bunch half length of $0.202m$ and $\Delta E/E_0 = 24.8 \cdot 10^{-5}$ at the initial energy.

Let us now choose the middle of the East section as the starting point and select on each 2-dimensional orbital plane (x, P_x), (y, P_y) and (z, P_z) four points with phases 0°, 90°, 180° and 270° on the perimeters of the invariant ellipses[4] corresponding to the chosen emittances.

For the numerical modelling of the acceleration cycle we have taken three sets of initial conditions as described below

- **Variant "xyz"**: six dimensional vectors of the initial orbital coordinates are constructed from all possible combinations of the two dimensional vectors described above. This gives us $4 \times 4 \times 4 = 64$ different particles in total.
- **Variant "xy0"**: this variant is obtained by setting the longitudinal coordinates of particles from the variant "xyz" to zero. This gives us 16 different particles.
- **Variant "0y0"**: setting the horizontal coordinates of the particles from the previous variant equal to zero, this last combination consists of 4 different particles only.
- The spins of all particles in all variants are initially set vertical.

[3] Note that on rotation by 180° this snake configuration will coincide with the snake configuration proposed in [4] (except for necessary shifts to the nearest free drift space). This was one additional reason to choose this model for a first simulation.

[4] These are the invariant ellipses following from the linear theory of the orbital motion.

6.3 The Behaviour of Orbital Oscillations

The computer tracking simulation of the acceleration cycle in HERA-p requires an enormously large number of turns (more then 10^8 turns) and it is not easy to check if our calculations still give reasonable results. One of the things which we checked periodically was the so called adiabatic damping of orbital oscillations during acceleration.

Figure 1 shows the projections of the coordinates of particles from the variant "xyz" on the horizontal and vertical planes at various values of the energy of the reference particle $E_0 = 40,\ 60,\ 90\ GeV$. Solid ellipses were drawn in accordance with linear adiabatic damping theory. We see that the decrease of the transverse emittances in our tracking simulation follows theoretical predictions very well. We note also that at the initial energy $40GeV$ (largest ellipses in the top and bottom pictures of figure 1) the particle projections form four groups due to our choice of initial conditions, and that for large energies (smaller ellipses) the phases of the particles spread apart so that each particle can be seen individually. This spreading of the phases is due to both the nonlinear coupling of the transverse coordinates and to the longitudinal motion. That there is a phase spread in the transverse motion due to the longitudinal motion can be seen by comparing the upper plot (variant "xyz") in figure 2 with the lower (variant "xy0"), which describes purely transverse motion.

Because the bunch length at the initial energy was chosen to be much smaller then the size of the separatrix, projections of coordinates of particles on the longitudinal plane were compared also with linear theory and the agreement (see figure 3) seems to be quite good too (at least up to $90\ GeV$). On this figure we see also how coupling with transverse oscillations affects the phases of the longitudinal motion.

6.4 The Real Acceleration Rate

We have not yet reached the top energy $820\ GeV$ in our tracking simulations of the acceleration cycle in HERA-p with the real acceleration rate, so we shall show currently available results which are:

- variant "xyz": up to $\approx 97\ GeV$
- variant "xy0": up to $\approx 190\ GeV$
- variant "0y0": up to $\approx 497\ GeV$

Figures 4-7 present a comparison of the behaviour of the spin motion in the energy range from 40 GeV to 100 GeV for all three variants of the initial conditions. Here and further on, we present the spin motion in terms of the ensemble averages along the $\vec{n}_0$ axis

$$\langle \vec{s} \cdot \vec{n}_0 \rangle = \frac{1}{N} \sum_{k=1}^{N} \vec{s}_k \cdot \vec{n}_0$$

where N is the number of particles in each variant and $\vec{n}_0$ is the value of the vector $\vec{n}_0(\tau, \gamma_0)$ at the middle of the East section at the corresponding energy (recall that for the configuration of snakes considered, $\vec{n}_0$ is vertical at all times). Note that figures 4-7 are drawn with the same vertical scale. To show more detail, in figure 8 we redraw figure 6 with a magnified vertical scale. The regions where the polarization falls correspond (more or less) to resonance between the spin and the vertical betatron motion. We see that the polarization recovers after acceleration through these regions. For the variant "0y0" the polarization shows a fine oscillatory structure but on including the horizontal and longitudinal motion, this structure is washed out and the curves become smoother. The effect of horizontal and vertical motion cannot therefore be ignored even at these energies.

Figures 9-10 show the behaviour of the spin motion in the energy range from 100 GeV to 190 GeV for the variants "0y0" and "xy0". The 'washing out' is seen here too.

Because for higher energies we have tracking results only for variant "0y0" we plotted these together with the strengths of the linear intrinsic spin resonances for betatron oscillations. For the resonance strengths the ring calculated is nonplanar without vertical bends in the East section and without any snakes. See figures 11-13. There is an obvious good match between the regions of strong depolarization disturbance and large resonance strength. Note that in figure 12 the resonance strengths are zero in the energy interval between 350 GeV and 360 GeV. This is not some defect in the calculations but a reflection of the complicated behaviour of spin tune in nonflat rings. Figure 14 shows the spin tune in zeroth approximation with respect to orbital oscillations. Recalling that the fractional parts of betatron tunes for our ring model are 0.28006 and 0.2723 we see that we really do not have linear resonances between spin and transverse orbital motions in that energy region. There is hardly any fall in the maximum polarization up to full energy.

Besides advancing continuously from 40 to 820 GeV we tracked particles with the real acceleration rate for some narrow high energy intervals. One

example of such investigations can be found on figure 15. Initial conditions for the particles were chosen in the same way as for the main calculations but with emittances decreased in accordance with linear adiabatic damping theory. Again there is hardly any fall in the maximum polarization.

Note that the measured longitudinal emittance at the energies considered in figure 15 (from 801.8 GeV to 805.5 GeV) is larger than the prediction of linear single particle theory (in the variables z and P_z). To look at the effect of the longitudinal motion on the spin motion at high energies, we have taken the increased value of the longitudinal emittance $\varepsilon_z = 0.08\,eV \cdot s$ for the calculation of the variant "xyz". The consequences of this may be seen in figure 16. It is clear that to obtain a complete picture all three orbital modes must be included, and that snakes are not always capable of suppressing the effects of longitudinal motion.

7 Increased Acceleration Rate

The enormous number of turns required for the numerical simulation of acceleration in HERA-p with more or less real values of the acceleration rate makes it impossible to make a systematic detailed tracking study of different snake configurations and seeds for misalignments. So for preliminary investigations we decided to use an increased acceleration rate and to take into account only the influence of the transverse oscillations on the spin motion. The increased acceleration rate was chosen to be constant during the ramp with a value $4\ MeV/turn$ (this is the lowest value that gives reasonable calculation times).

7.1 Comparison with Real Ramping Speed

The three figures 17-19 show the behaviour of the spin motion for the real and for the increased ramping speed (figure 18 is a part of figure 17 drawn with a magnified horizontal scale for a smaller energy region). The level of agreement looks quite reasonable and in all further calculations we shall use an acceleration rate of $4\ MeV/turn$ and shall not take into account synchrotron oscillations.

7.2 Tracking with Increased Ramping Speed

The upper part of the figure 20 shows the result of simulations of the whole acceleration cycle for particles which oscillate only vertically. On the lower part of this figure we additionally took into account horizontal motion. For the chosen emittances (1σ) the difference in the spin behaviour is almost invisible.

Before proceeding further we wish to show with the help of figure 21 that (as in [1]) the results of our calculations do not change significantly with an increase in the number of particles. Unfortunately we were not able to check this with 1000 particles (unlike [1]) because it destroys all the advantages we have obtained by increasing the ramping speed.

Figure 22 shows the difference in the spin motion for HERA-p with and without flattening snakes. The four flattening snakes apparently contribute little to the maintenance of polarization.

7.3 Increased Transverse Emittances

All previous calculations were made for values of transverse emittances not more then 1σ. We now introduce the notation "XY0" and "0Y0" for two sets of initial conditions which are formed with the help of the same rules as for the initial conditions from the variants "xy0" and "0y0" with the exception that the values of transverse emittances are taken now to be $\varepsilon_x = \varepsilon_y = 16 \cdot 10^{-6} mrad$. This value corresponds to the 2σ beam size.

Figures 23-24 show that with the snake configuration considered this increase of emittances has dramatic consequences for the spin motion above $400\,GeV$ and that with horizontal motion the difficulties begin earlier.

8 The Effect of Spin Matching

"Spin matching" is a localized compensation scheme for linear spin-orbit coupling which produces spin transparency at the linear level for the ring as a whole, or for some of its subsections (see, for example [20]).

In this section we shall show some preliminary results of a study of the effect of spin matching on the behaviour of proton spin motion in HERA-p.

We shall use the simplest possible localized compensation technique, namely a special choice of betatron and spin tunes per cell in a ring which consists of n identical cells. Because we wish to eliminate the linear coupling

between the spin and transverse orbit motion over a large range of energies, we have to equip each cell with snakes to stabilize the spin tune to some constant value.

The idea for the first check was to consider one turn around HERA-p as one cell and thus our "n cell ring" consists of n turns around HERA-p. Taking $n = 4$ we slightly changed the strengths of the quadrupole components of the combined function magnets (QP40 and QP42) in the arcs to reach values of the betatron tunes $Q_x = 31.25$ and $Q_y = 32.25$. Then we placed one full longitudinal snake in the free space near the West IP and one full radial snake near the North, South and East IP's respectively (i.e. our basic configuration of snakes) to obtain a spin tune of 0.5 in zeroth approximation with respect to orbital oscillations.

Let us now introduce one and four turn maps

$$\vec{s}_1 = A_1(\vec{u}_0)\,\vec{s}_0$$

$$\vec{s}_4 = A_4(\vec{u}_0)\,\vec{s}_0$$

where $\vec{u}_0$ contains the initial values of the orbital variables, $\vec{s}_0$ is the initial value of the spin vector, and $\vec{s}_1$ and $\vec{s}_4$ are the values of the spin vector after one and four turns respectively.

To illustrate that with chosen orbital and spin tunes we do not have 1-turn spin matching, but have nevertheless reduced the effect of the transverse orbital oscillations on the spin motion in the 4-turn map, we print below components of some of the elements of the matrices A_1 and A_4 in linear approximation with respect to the transverse orbital variables [5].

$$\begin{aligned}(A_1)_{1,1} = & - 9.999985e-01 \\ & + 3.540912e-01 \cdot x - 4.589953e+00 \cdot P_x \\ & + 6.064381e+00 \cdot y - 1.128331e+01 \cdot P_y\end{aligned} \tag{3}$$

$$\begin{aligned}(A_4)_{1,1} = & + 9.999999e-01 \\ & - 7.694750e-08 \cdot x + 1.680937e-05 \cdot P_x \\ & + 3.207008e-07 \cdot y + 7.304348e-09 \cdot P_y\end{aligned} \tag{4}$$

[5]Note that these matrices where calculated for the energy 801.8 GeV and that this number was taken randomly.

$$
\begin{aligned}
(A_1)_{1,2} \;=\; & -\; 1.728907e-03 \\
& -\; 2.140665e+02\cdot x \;+\; 2.851027e+03\cdot P_x \\
& -\; 3.495204e+03\cdot y \;+\; 6.417311e+03\cdot P_y
\end{aligned}
\tag{5}
$$

$$
\begin{aligned}
(A_4)_{1,2} \;=\; & +\; 7.781352e-08 \\
& +\; 5.027224e-03\cdot x \;+\; 7.145043e-01\cdot P_x \\
& -\; 1.953356e-01\cdot y \;+\; 6.386367e-01\cdot P_y
\end{aligned}
\tag{6}
$$

Note that according to theory, in the functions $(A_4)_{1,1}$ and $(A_4)_{1,2}$ the multipliers in the front of transverse coordinates should not only be small but should be exactly zero. This does not happen because our spin tune is not exactly 0.5 and is even slightly energy dependent due to weak vertical bends which are installed near the West IP and which break the mirror symmetry (see more details in [1]), and also because the real betatron tunes which we obtain by changing the strengths of the quadrupole components of the combined function magnets QP40 and QP42 have fractional parts slightly different from 0.25:

$$
Q_x \;=\; 31.2499509, \qquad Q_y \;=\; 32.2500371 \tag{7}
$$

Are we ready now to start tracking simulations? Not yet, because with the chosen values of tunes we have placed ourselves exactly on a nonlinear spin-orbit resonance and the consequences of this can seen in the upper part of figure 25. To avoid the effect of nonlinear resonances we constructed a new "ring" which consists of four turns around the HERA-p ring plus one snake with a vertical axis. This snake was chosen to obtain a fractional part of the spin tune for the new structure equal to 0.17 and it was a somewhat random choice[6]. The tracking result can be seen at the bottom of the figure 25.

It is clear that the situation improved in comparison with the bottom of the figure 22, but, even with such small defects in the values of the spin and betatron tunes, we were not able to avoid completely the local drops of polarization at some energies. Calculating the 4-turn map for the energy

[6]We left the orbital tunes equal to each other because for this first check we used linear uncoupled motion model for the orbital tracking.

804.6 GeV which corresponds to one such local drop of polarization and printing out $(A_4)_{1,1}$ and $(A_4)_{1,2}$ for that particular energy

$$\begin{aligned}(A_4)_{1,1} \;=\; &+\; 9.999967e-01 \\ &+\; 4.100821e-07\cdot x \;-\; 1.468152e-04\cdot P_x \\ &-\; 2.179490e-06\cdot y \;-\; 1.756586e-04\cdot P_y\end{aligned} \tag{8}$$

$$\begin{aligned}(A_4)_{1,2} \;=\; &-\; 1.646510e-06 \\ &-\; 6.995868e-02\cdot x \;+\; 9.433438e+00\cdot P_x \\ &+\; 1.245922e+00\cdot y \;-\; 5.774516e+01\cdot P_y\end{aligned} \tag{9}$$

we see a significant increase of the linear coupling to orbital oscillations in (8) and (9) in comparison with (4) and (6) respectively.

Note that for the 4-turn spin matching we can use fewer than four snakes. Some examples with one, two and four full snakes in the ring and with one additional snake for every four turns are shown on figure 26. Even with only one snake the polarization is maintained up to a resonance at 400 GeV and with two snakes one can reach about 600 GeV.

8.1 One Turn Spin Matching

HERA-p has approximate four-fold symmetry. To improve this symmetry we take one quarter of HERA-p (from the middle of the arc between the North and East IP's up to the middle of the arc between the East and South IP's) and we construct the new ring by repeating this four times. Then we again slightly changed the strengths of the quadrupole components of the combined function magnets (QP40 and QP42) to obtain betatron tunes for one quarter to be very close to the values $Q_x = 7.75$ and $Q_y = 8.25$ instead of the old values $Q_x = 7.6880$ and $Q_y = 8.3498$. So we obtained a flat four-fold symmetric ring[7].

If now we take a full snake with an arbitrary rotation axis lying in the horizontal plane and then place identical copies of this snake in the North, East, South and West, we obtain a ring which gives us one turn spin matching.

To avoid spin-orbit resonances we placed one additional vertical snake in the middle of the arc between the North and East to make the fractional part

[7]Of course, the same can be done with a quarter which contains vertical bends, but in this paper we demonstrate only the flat model.

of the spin tune equal to 0.17 (as in our 4-turn spin matching example). To avoid orbit resonances (now we return to using of our standard model orbital motion) we installed at the same place a thin lens element which changes the betatron tunes back to the usual values $Q_x = 31.28032$ and $Q_y = 32.2723$.

The tracking results for four full radial snakes and for four full longitudinal snakes are shown in figure 27 for the variant "0y0". The increase of the emittance to the 2σ beam size (the variant "0Y0") has dramatic consequences for the spin motion (see the bottom picture of figure 28) and although there is a strong loss of polarization at about $500\,GeV$ the polarization nevertheless almost recovers between $700\,GeV$ and $800\,GeV$. The spin dynamics in the presence of this kind of spin matching is clearly very subtle and very differennt from that in figure 23.

9 Some Conclusions

Since it would be very difficult in practice to insert snakes at the midpoints of the arcs we believe that we should continue the study of the question: "Is it possible to accelerate a polarized proton beam in HERA-p without significant loss of polarization using only additional devices which can be placed in straight sections?"

The tracking results of this paper give us the hope that this is possible, because in the framework of the model considered without misalignments and with increased acceleration rate (and without longitudinal oscillations) sufficient polarization remains at the end of the acceleration cycle and this value can be significantly improved by spin matching.

As the two currently important problems we would like to mention the problem of the stability of the recovery of the polarization to its initial value after a local drop at some energies [8] and the study of how to overcome the effect on spin motion of misalignments. A lot of work in both directions is already in progress.

[8] In our opinion this problem of local drops cannot be solved completely just by a reasonable increase in the number of snakes. Some example are shown in figures 29-30, where we increased the number of full snakes in the ring, but, in truth, without any optimization of snakes parameters.

References

[1] Balandin, V.V., Golubeva, N.I., Barber, D.P., *Studies of the Behaviour of Proton Spin Motion in HERA-p at High Energies*, DESY M 96-04, (1996).

[2] Barber, D.P. et al., *The first Achievement of Longitudinal Polarization in a high Energy Electron Storage Ring*, Physics Letters, B343: 436, (1995).

[3] Barber, D.P., *Possibilities for polarized protons at HERA*, In *Prospects of spin physics at HERA*, DESY-Zeuthen, August 1995, DESY Report 95-200, November 1995.

[4] SPIN Collaboration and DESY Polarization Team, *Acceleration of Polarized Protons to* 820 *GeV at HERA*, UM-HE 96-20, 1996.

[5] Balandin, V.V., Golubeva, N.I., *Siberian Snakes for Nonflat Rings with Symmetries*, unpublished notes, July 1995.

[6] Thomas, L.H., *Philos. Mag.*, **3**:1, (1927).

[7] Bargmann, V., Michel, L., and Telegdi, V.L., *Precession of the polarization of particles moving in a homogeneous electromagnetic field*, Phys. Rev. Lett., 2(10):435-436, (1959).

[8] Balandin, V.V., Golubeva, N.I., *Nonlinear Spin Dynamics*, Proc. XV Int. Conf. High Energy Accelerators, Hamburg, 1992, Int. J. Mod. Phys. A, **2B**: 998, (1992).

[9] Balandin, V.V., Golubeva, N.I., *Investigation of Spin Motion in the Booster Lattice*, TRIUMF Report TRI-DN-93-K236, (1993).

[10] Balandin, V.V., Golubeva, N.I., *Polarized Protons in HERA. Part B: Studies of Spin Motion at High Energy in HERA*, Proceeding of the 3rd Meeting on the Prospects of Nucleon-Nucleon Spin Physics at HERA, Dubna, (1996).

[11] Courant, E.D., Ruth, R.D., *The Acceleration of Polarized Protons in Circular Accelerators*, BNL 51270 (1990).

[12] Balandin, V.V., Golubeva, N.I., *Hamiltonian Methods for the Study of Polarized Proton Beam Dynamics in Accelerators and Storage Rings*, DESY report DESY 98-16 (1998).

[13] Balandin, V.V., Golubeva, N.I., *Taylor Maps and Calculations of Equilibrium Polarization Direction for Proton Storage Rings*, Particle Accelerator Conference, Washington, USA, (1993).

[14] Balandin, V.V., *One of Methods to Extract Truncated Taylor Map for Orbital and Spin Motion in Proton Storage Rings*, Particle Accelerator Conference, Washington, USA, (1993).

[15] Balandin, V.V., Golubeva, N.I., *Hamiltonian Methods for the Study of Polarized Proton Beam Dynamics in Accelerators and Storage Rings*, Computational Accelerator Physics Conference, Williamsburg, Virginia, USA, (1996).

[16] Balandin, V.V., Golubeva, N.I., *Fast Betatron Tune Jumps and Partial Siberian Snakes for Preserving the Polarization in the Booster Lattice*, TRIUMF Report TRI-DN-93-K240, (1993).

[17] Balandin, V.V., Chursin, A.G., Dubinsky, G.A., Esin, S.K., Golubeva, N.I et al., *The proposal of the Accelerator Complex of the Moscow Kaon Factory*, Proc. of 14th Biennial IEEE Particle Accel. Conference, May 6-9, 1991, San Francisco, CA, USA.

[18] Balandin, V.V., Senichev, Yu. V., *Space Charge Effect in Crossing of Third Order Resonance*, EPAC, London, (1994).

[19] Kondratenko, A.M., Golubeva, N.I., *Depolarization of Proton Beam in the Nuclotron Ring at JINR*, VII Workshop on High Energy Spin Physics, Dubna, July 1997.

[20] Steffen, K., *Strong Spin Matching with and without Snakes, a Scheme for Preserving Polarization in Large Ring Accelerators*, DESY 88-068, May 1988. and Part.Accel., 24:45, (1988).

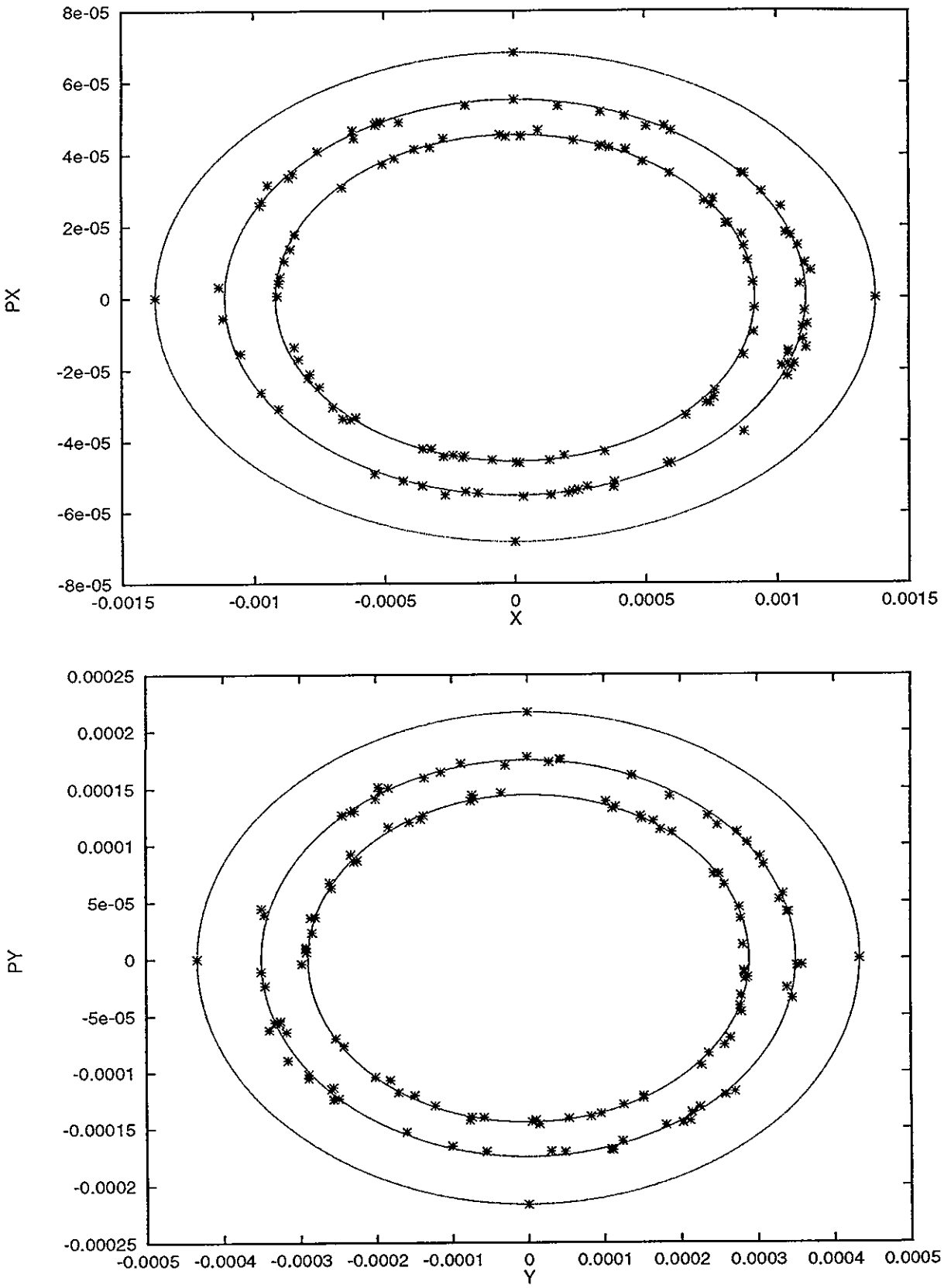

Figure 1: Projections of coordinates of particles from the variant *"xyz"* on the horizontal and vertical planes at different energies $E = 40,\ 60,\ 90\ GeV$.

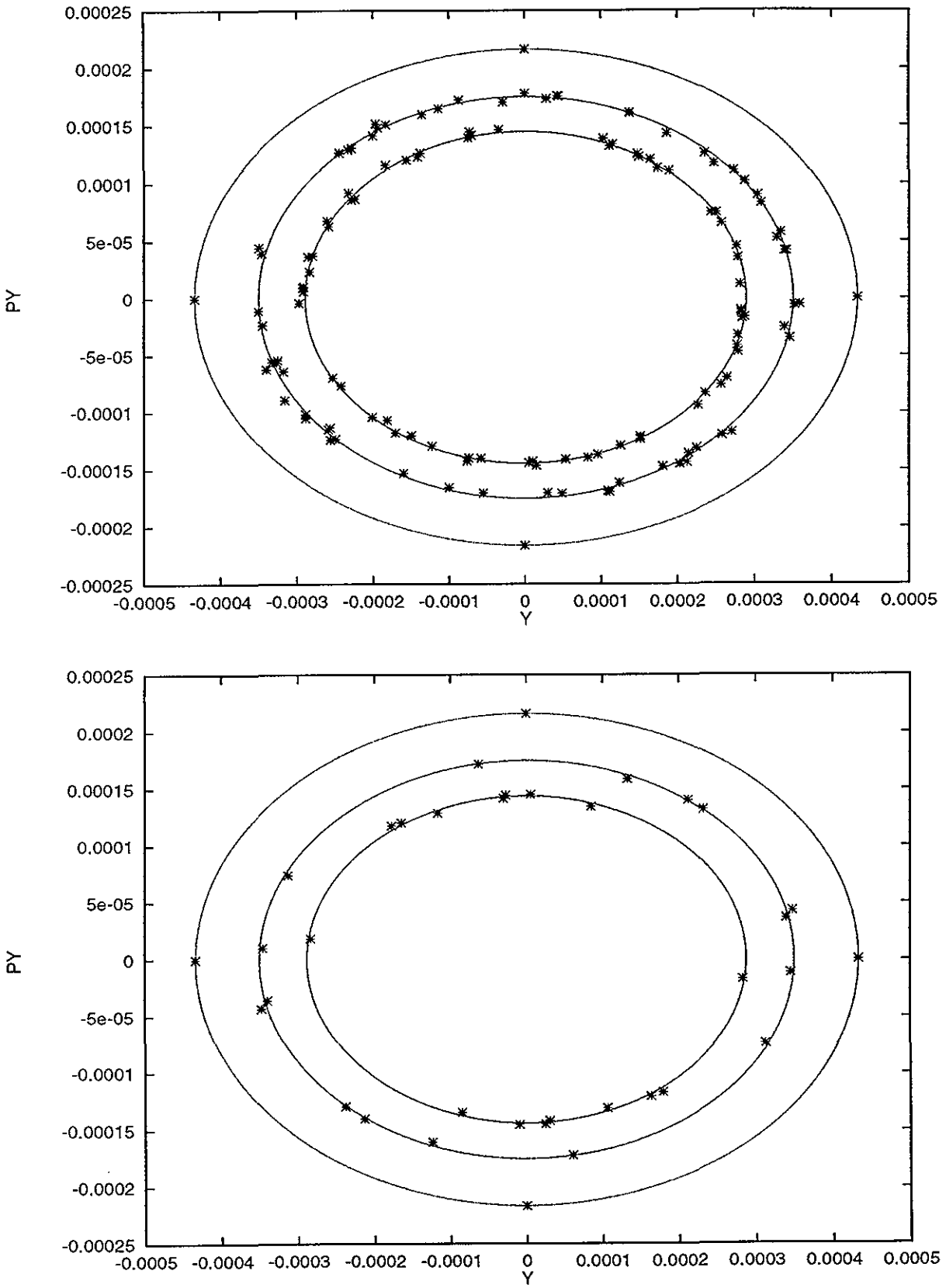

Figure 2: Projections of coordinates of particles on the vertical plane at different energies $E = 40, 60, 90\ GeV$. Top: particles from the variant "xyz". Bottom: particles from the variant "$xy0$".

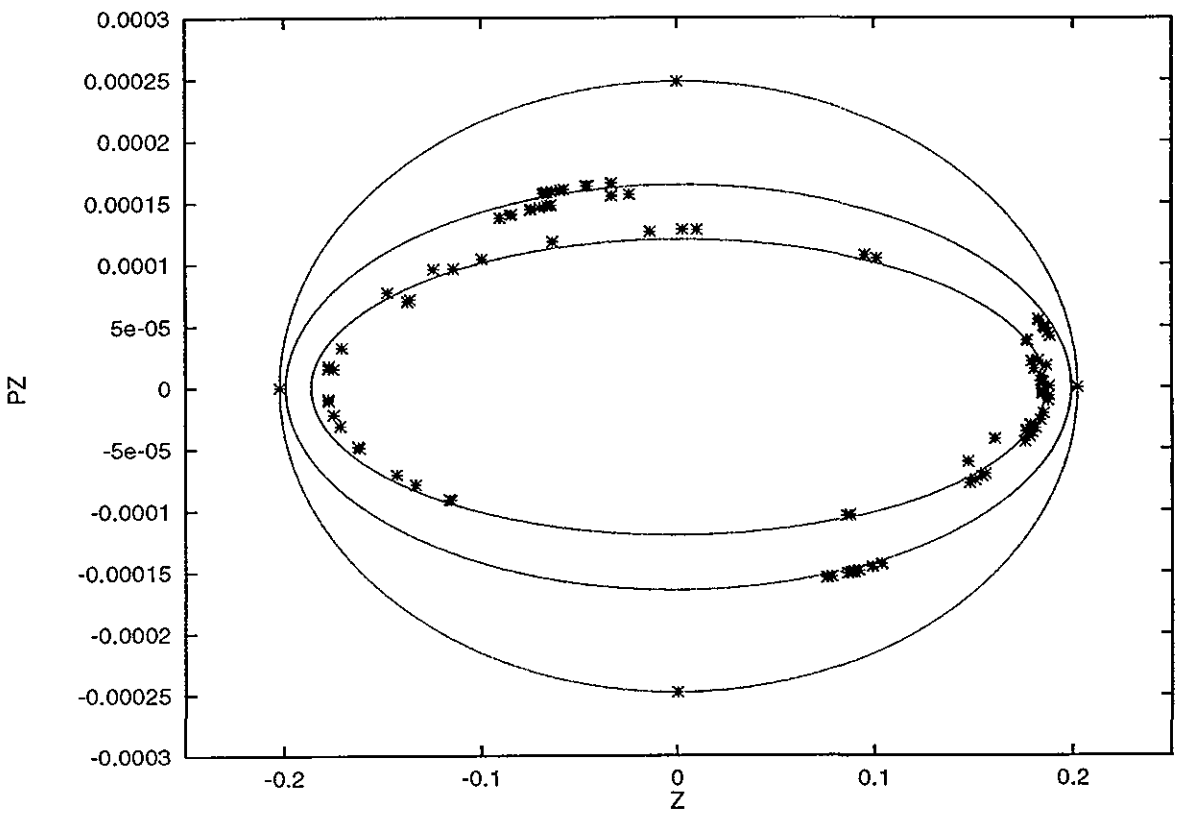

Figure 3: Projections of coordinates of particles from the variant *"xyz"* on the longitudinal plane at different energies $E = 40,\ 60,\ 90\ GeV$.

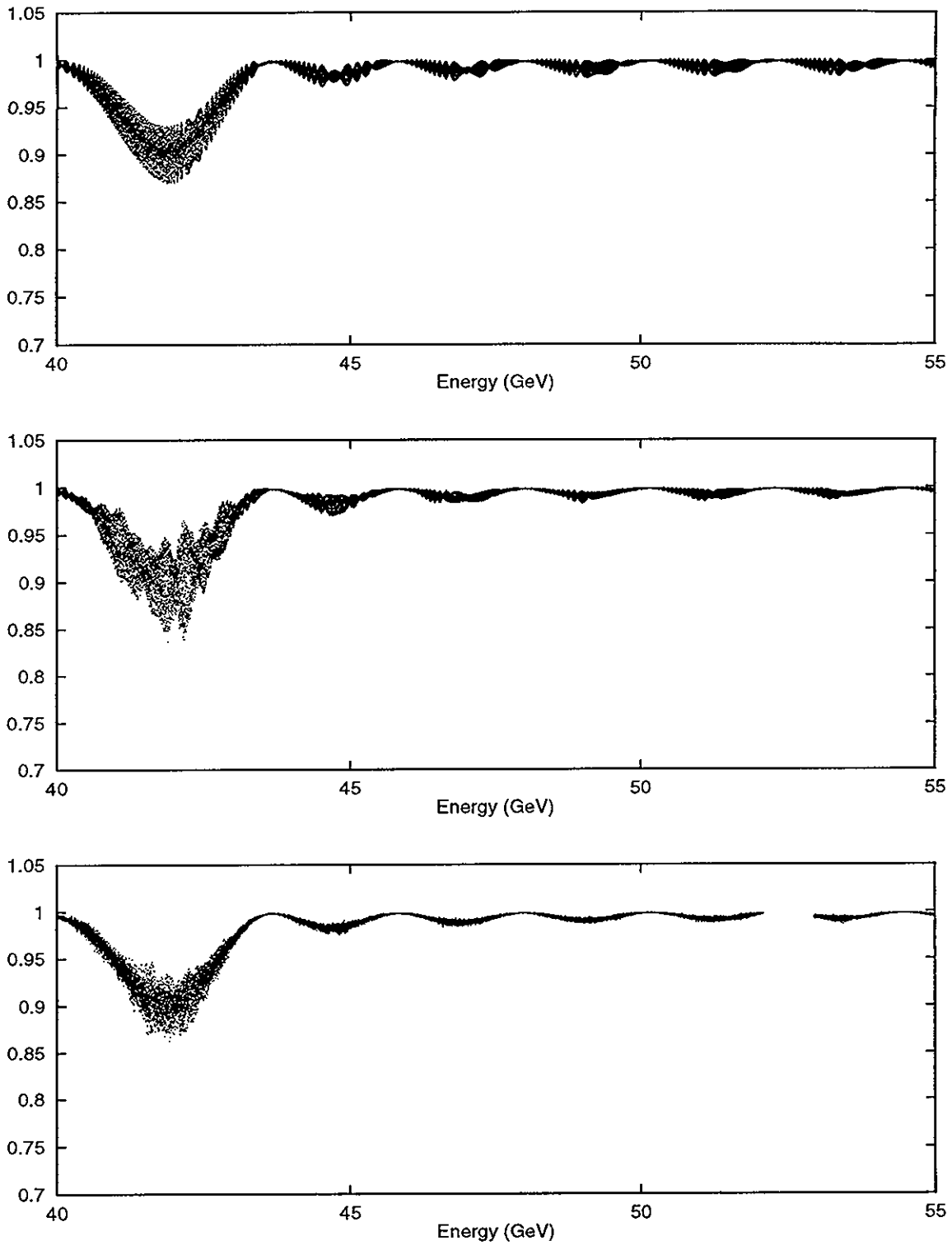

Figure 4: Behaviour of the spin motion during acceleration in HERA-p with 4 FS and 4 snakes (rrlr) and without vertical bends in the East section. Real acceleration rate. The view point is the East IP ($\langle \vec{s} \cdot \vec{n}_0 \rangle$). Top: the variant "$0y0$". Middle: the variant "$xy0$". Bottom: the variant "$xyz$".

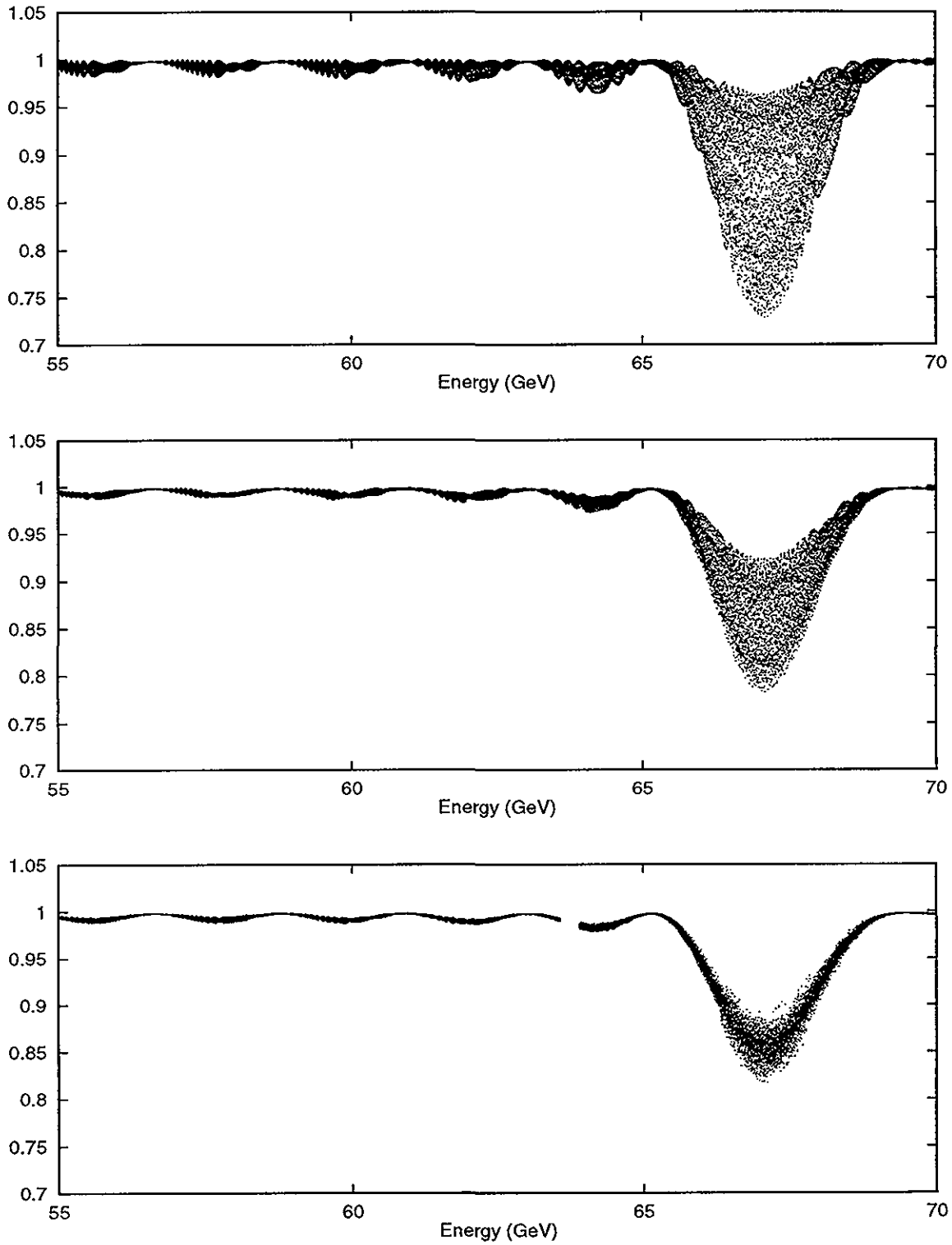

Figure 5: Behaviour of the spin motion during acceleration in HERA-p with 4 FS and 4 snakes (rrlr) and without vertical bends in the East section. Real acceleration rate. The view point is the East IP ($\langle \vec{s} \cdot \vec{n}_0 \rangle$). Top: the variant "$0y0$". Middle: the variant "$xy0$". Bottom: the variant "$xyz$".

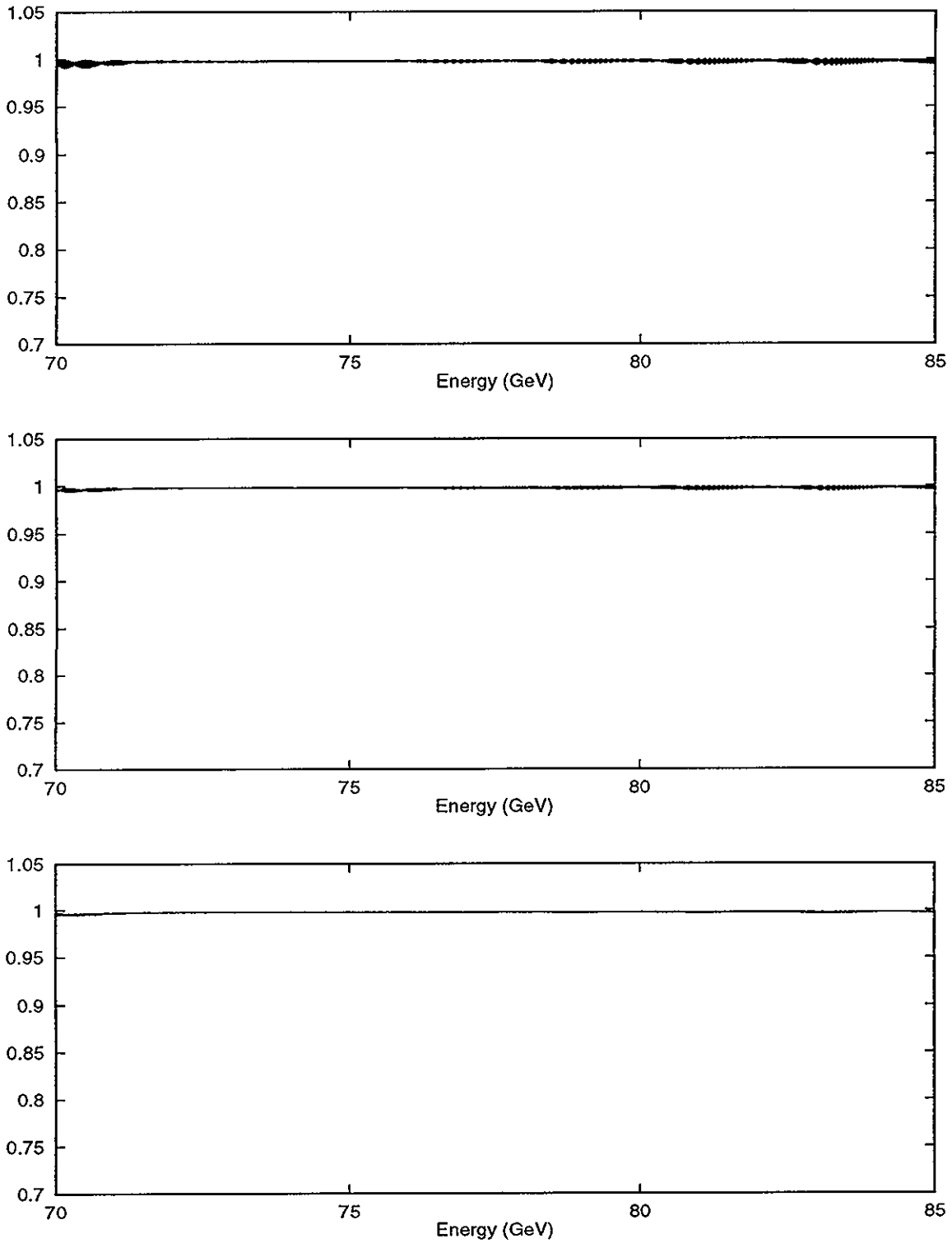

Figure 6: Behaviour of the spin motion during acceleration in HERA-p with 4 FS and 4 snakes (rrlr) and without vertical bends in the East section. Real acceleration rate. The view point is the East IP ($\langle \vec{s} \cdot \vec{n}_0 \rangle$). Top: the variant "$0y0$". Middle: the variant "$xy0$". Bottom: the variant "$xyz$".

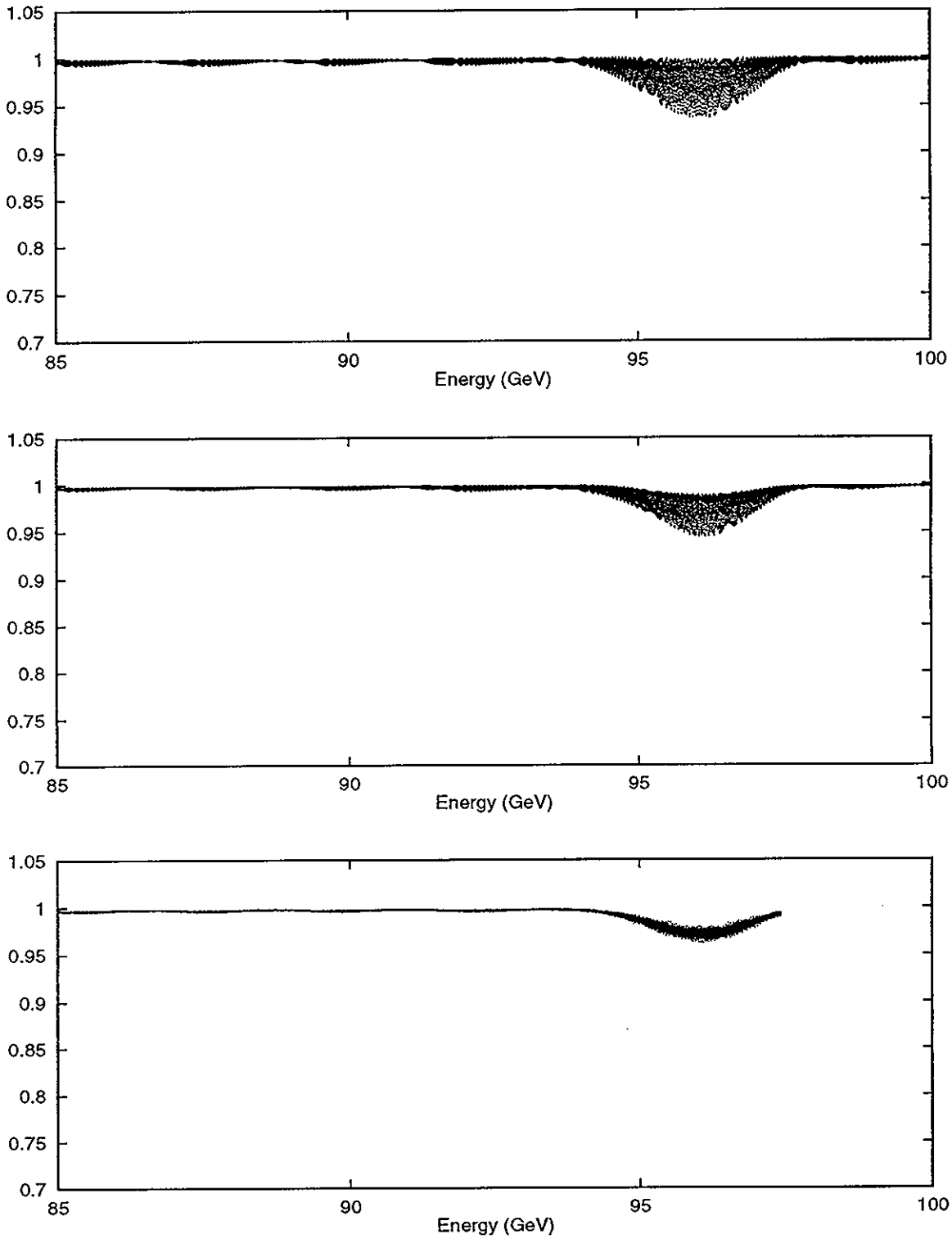

Figure 7: Behaviour of the spin motion during acceleration in HERA-p with 4 FS and 4 snakes (rrlr) and without vertical bends in the East section. Real acceleration rate. The view point is the East IP ($\langle \vec{s} \cdot \vec{n}_0 \rangle$). Top: the variant "$0y0$". Middle: the variant "$xy0$". Bottom: the variant "$xyz$".

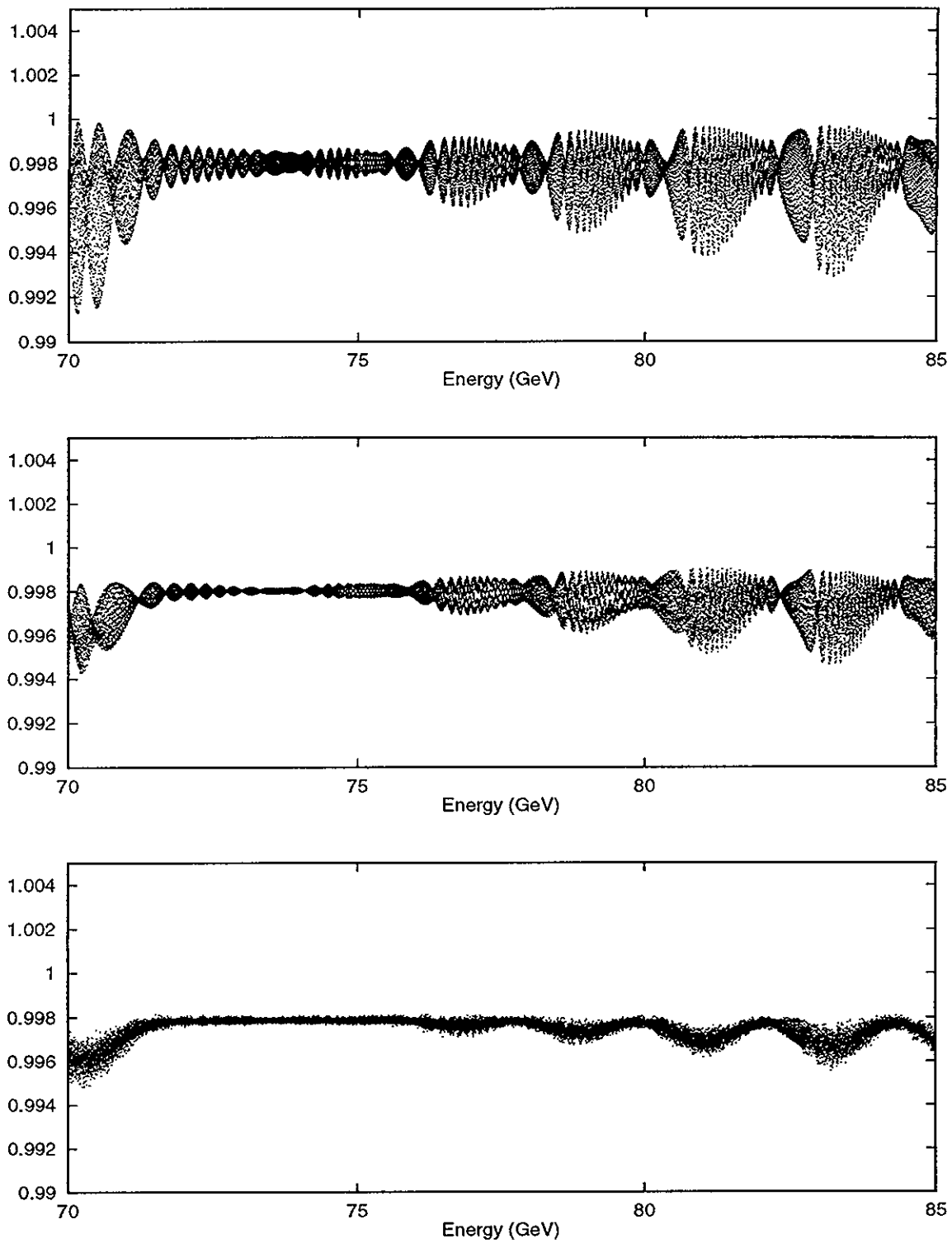

Figure 8: Behaviour of the spin motion during acceleration in HERA-p with 4 FS and 4 snakes (rrlr) and without vertical bends in the East section. Real acceleration rate. The view point is the East IP ($\langle \vec{s} \cdot \vec{n}_0 \rangle$). Top: the variant "$0y0$". Middle: the variant "$xy0$". Bottom: the variant "$xyz$".

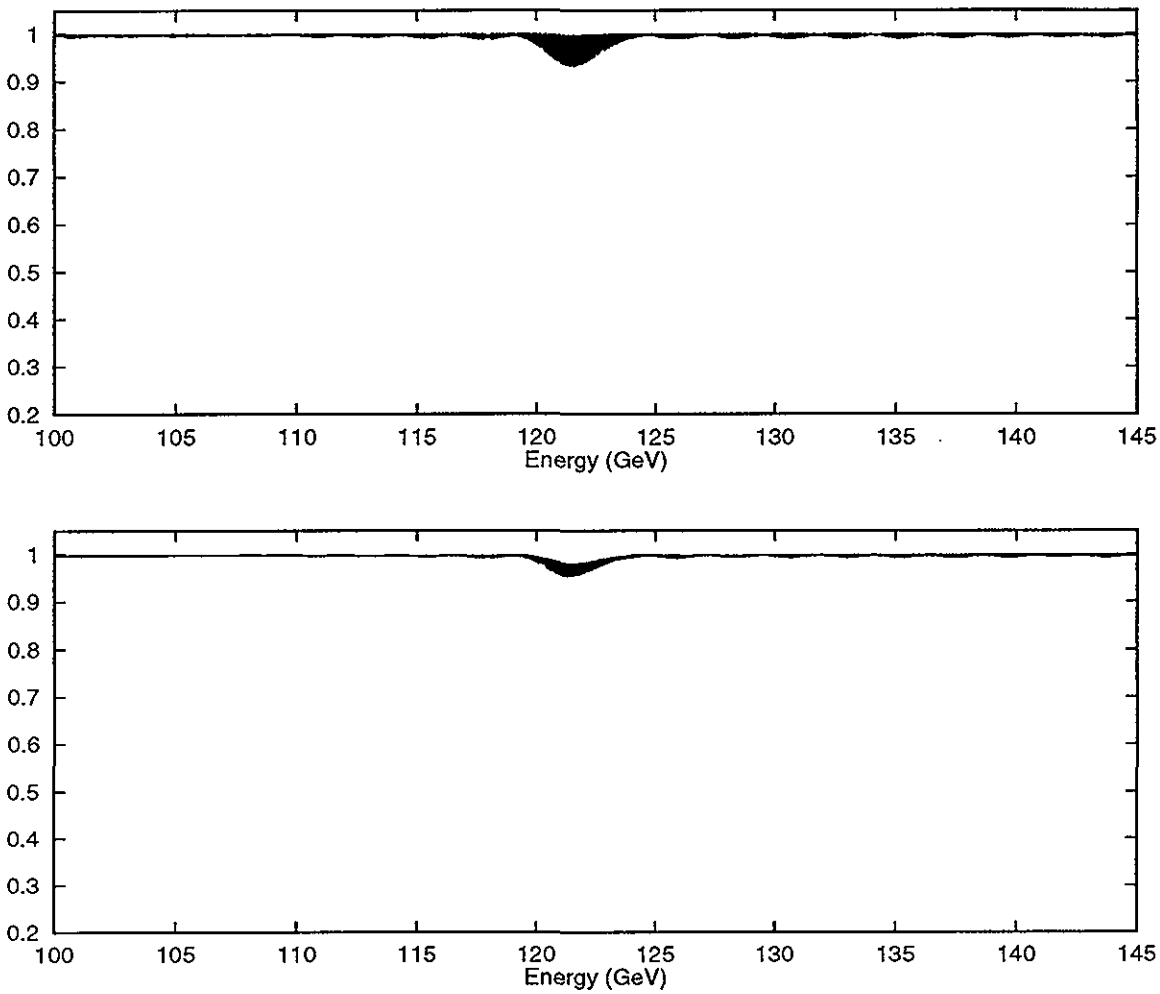

Figure 9: Behaviour of the spin motion during acceleration in HERA-p with 4 FS and 4 snakes (rrlr) and without vertical bends in the East section. Real acceleration rate. The view point is the East IP ($\langle \vec{s} \cdot \vec{n}_0 \rangle$). Top: the variant "$0y0$". Bottom: the variant "$xy0$".

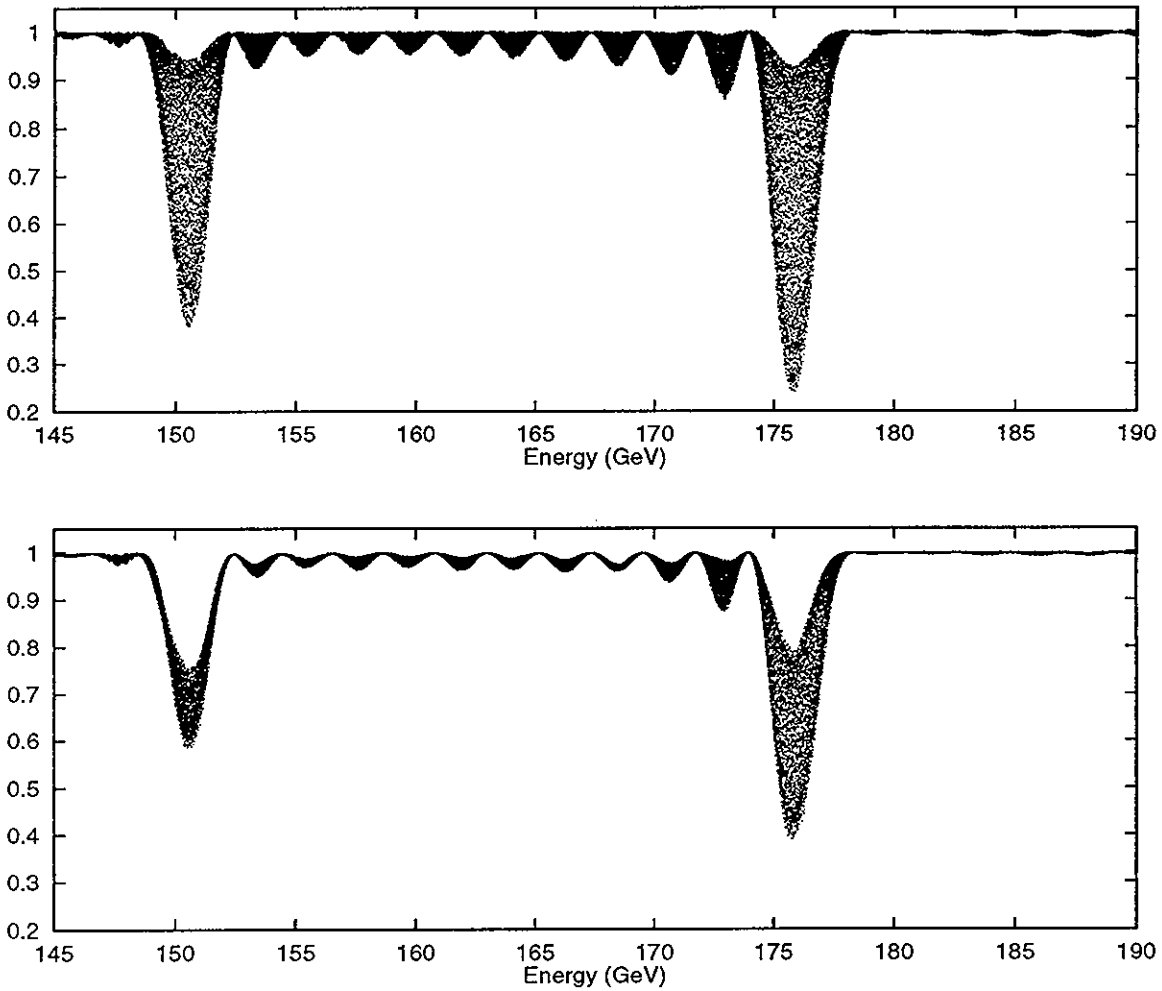

Figure 10: Behaviour of the spin motion during acceleration in HERA-p with 4 FS and 4 snakes (rrlr) and without vertical bends in the East section. Real acceleration rate. The view point is the East IP ($\langle \vec{s} \cdot \vec{n}_0 \rangle$). Top: the variant "$0y0$". Bottom: the variant "$xy0$".

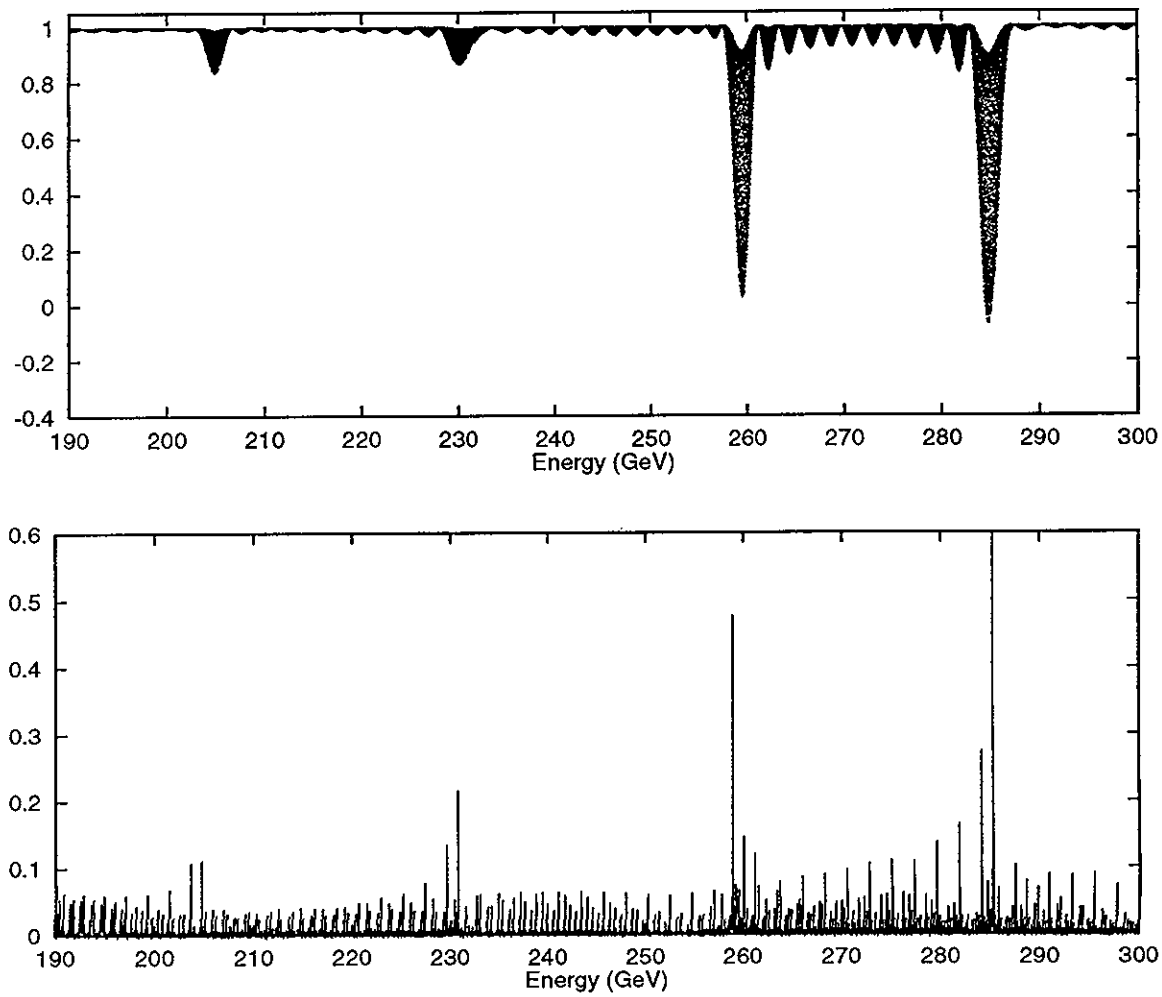

Figure 11: Top: behaviour of the spin motion during acceleration in HERA-p with 4 FS and 4 snakes (rrlr) and without vertical bends in the East section. Real acceleration rate. The view point is the East IP ($\langle \vec{s} \cdot \vec{n}_0 \rangle$). The variant "$0y0$". Bottom: strengths of linear intrinsic spin resonances with betatron oscillations calculated for nonplanar HERA-p without vertical bends in the East section and without snakes.

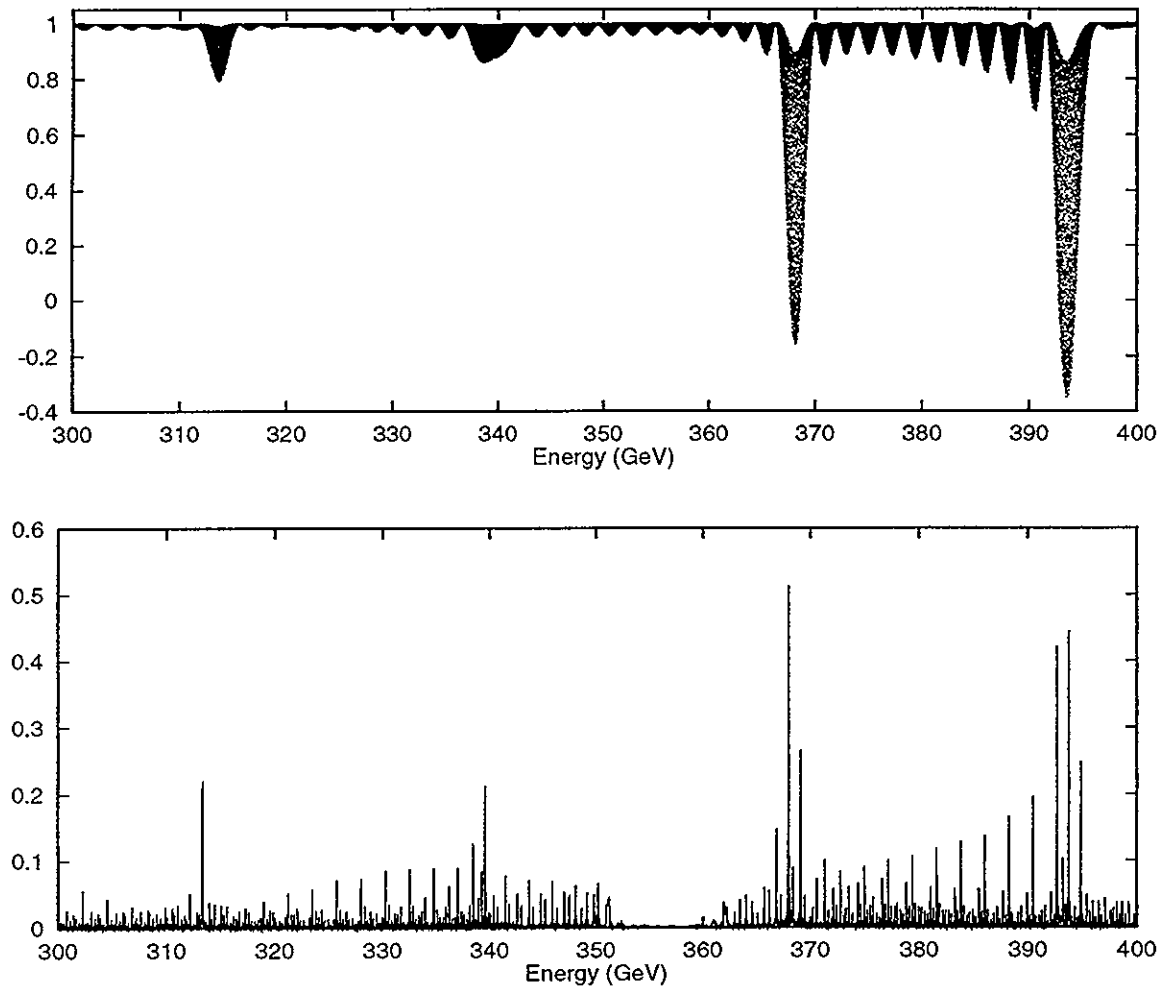

Figure 12: Top: behaviour of the spin motion during acceleration in HERA-p with 4 FS and 4 snakes (rrlr) and without vertical bends in the East section. Real acceleration rate. The view point is the East IP ($\langle \vec{s} \cdot \vec{n}_0 \rangle$). The variant "$0y0$". Bottom: strengths of linear intrinsic spin resonances with betatron oscillations calculated for nonplanar HERA-p without vertical bends in the East section and without snakes.

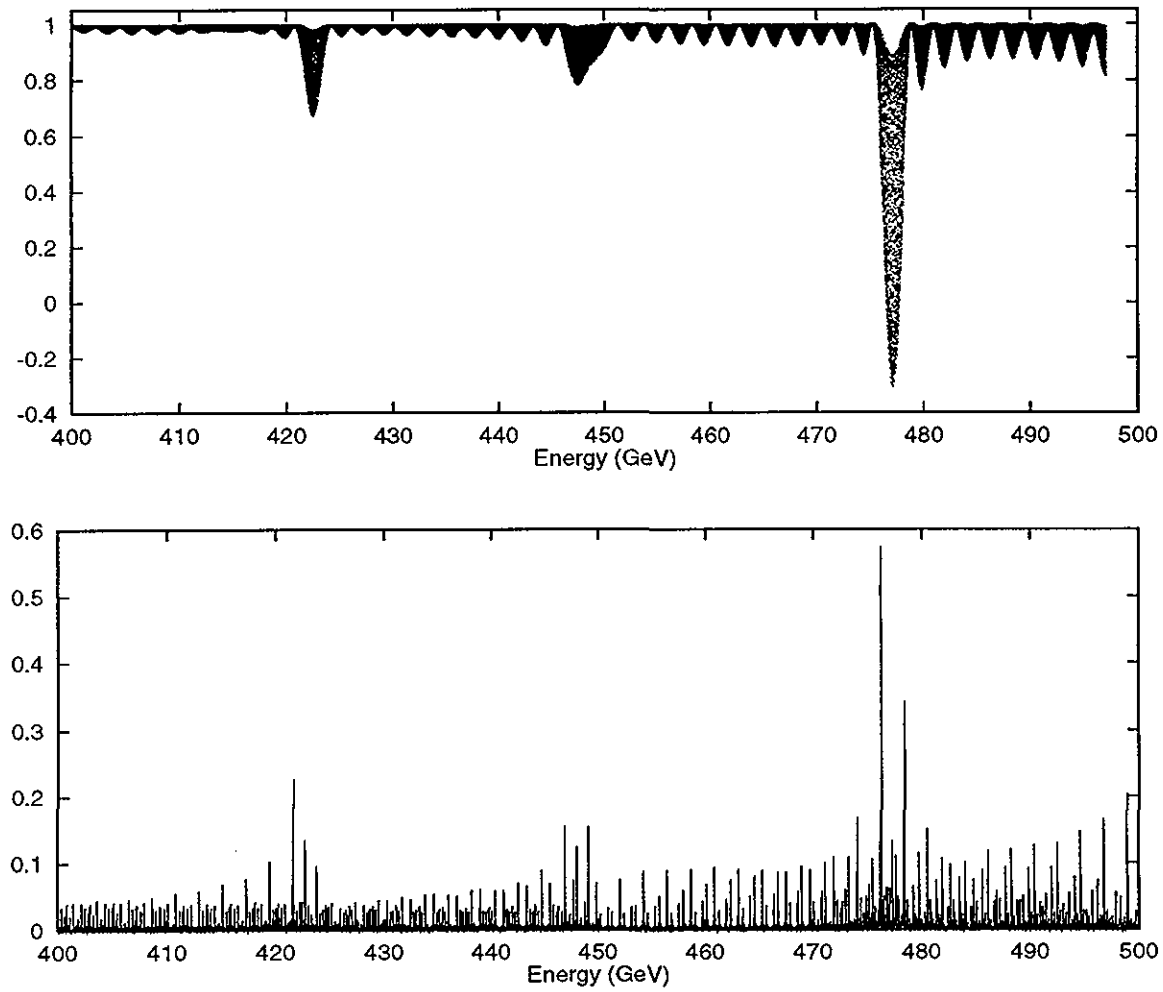

Figure 13: Top: behaviour of the spin motion during acceleration in HERA-p with 4 FS and 4 snakes (rrlr) and without vertical bends in the East section. Real acceleration rate. The view point is the East IP ($\langle \vec{s} \cdot \vec{n}_0 \rangle$). The variant "$0y0$". Bottom: strengths of linear intrinsic spin resonances with betatron oscillations calculated for nonplanar HERA-p without vertical bends in the East section and without snakes.

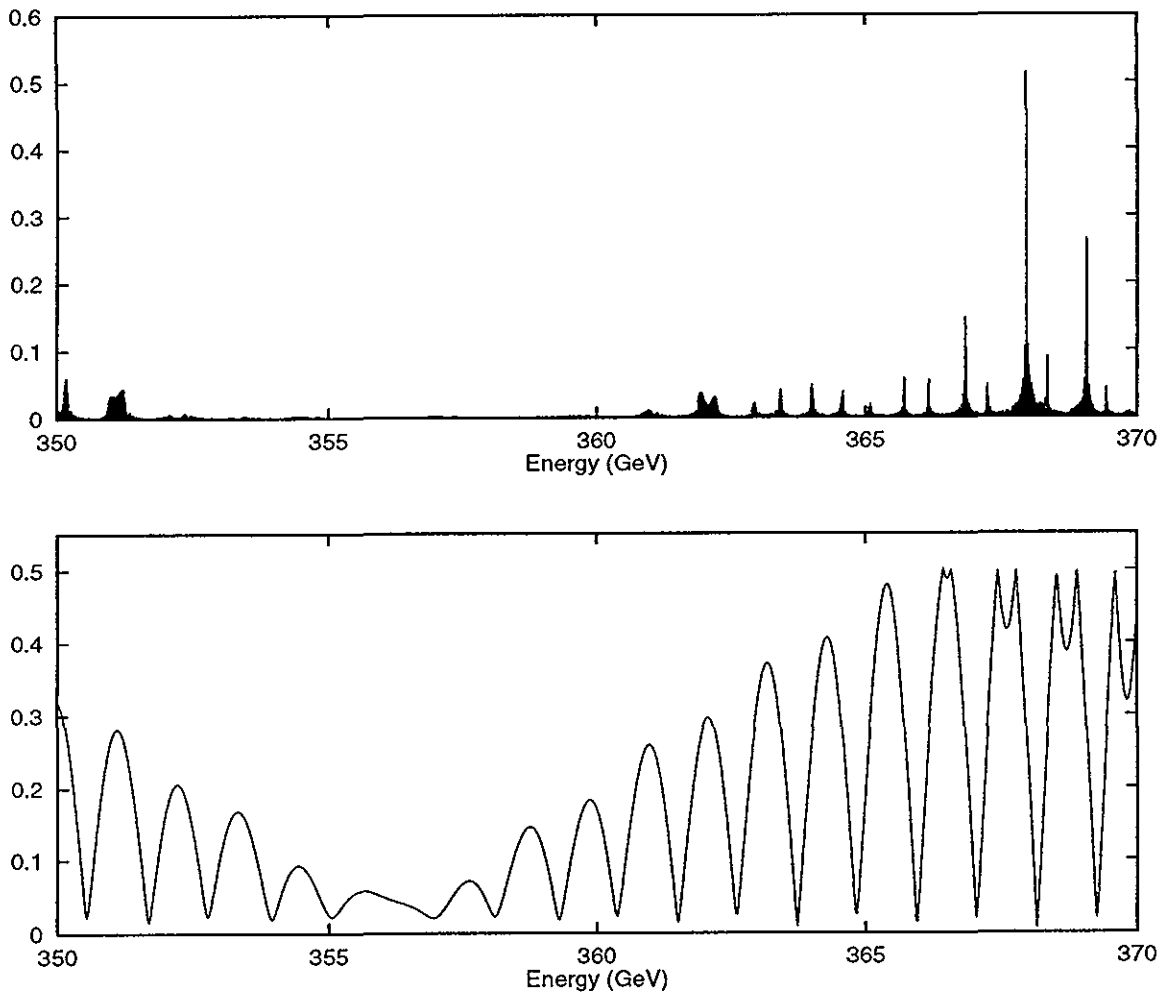

Figure 14: Nonplanar HERA-p without vertical bends in the East section and without snakes. Top: strengths of linear intrinsic spin resonances with betatron oscillations. Bottom: behaviour of the spin tune in zeroth approximation with respect to orbital oscillations.

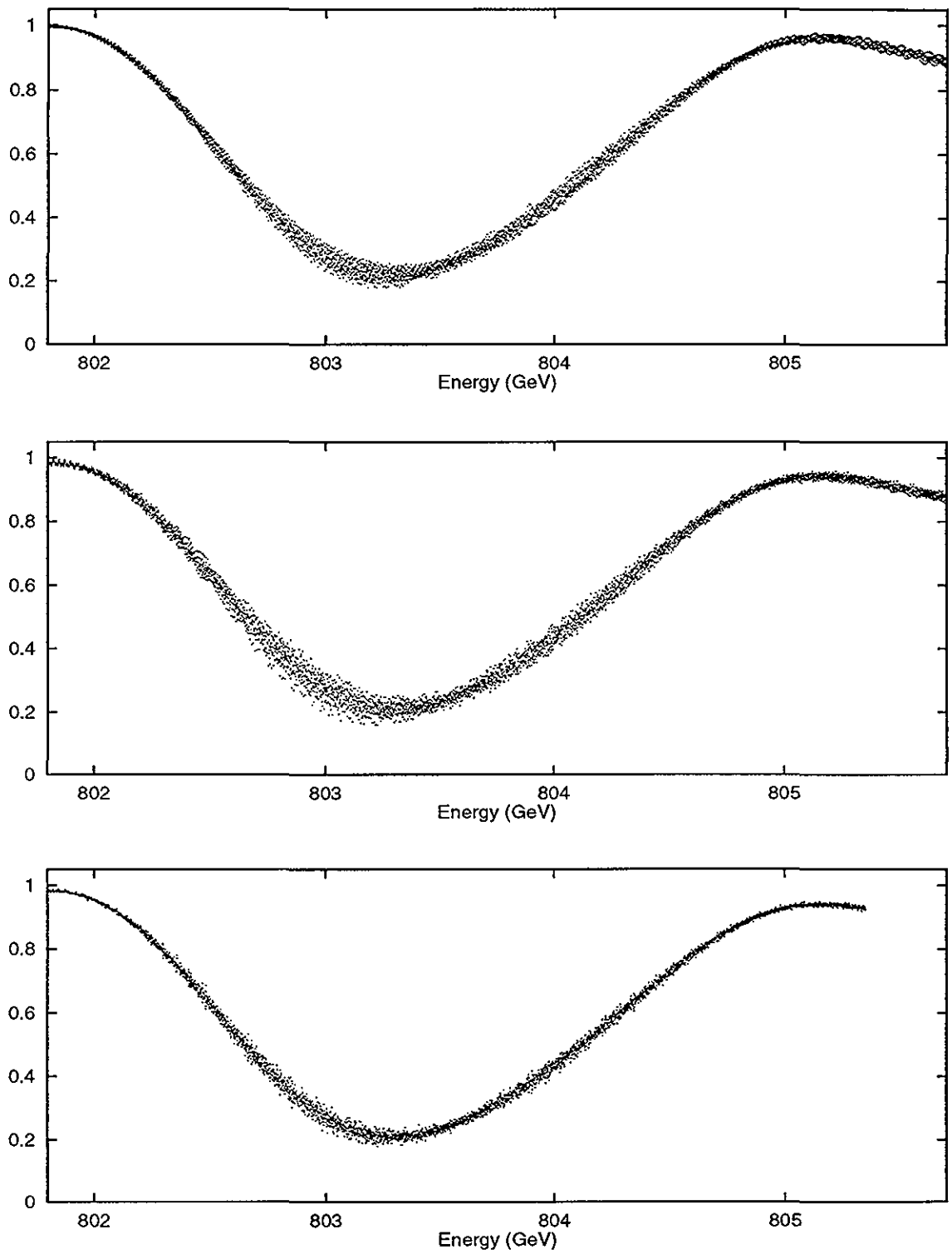

Figure 15: Behaviour of the spin motion during acceleration in HERA-p with 4 FS and 4 snakes (rrlr) and without vertical bends in the East section. Real acceleration rate. The view point is the East IP ($\langle \vec{s} \cdot \vec{n}_0 \rangle$). Top: the variant "$0y0$". Middle: the variant "$xy0$". Bottom: the variant "$xyz$".

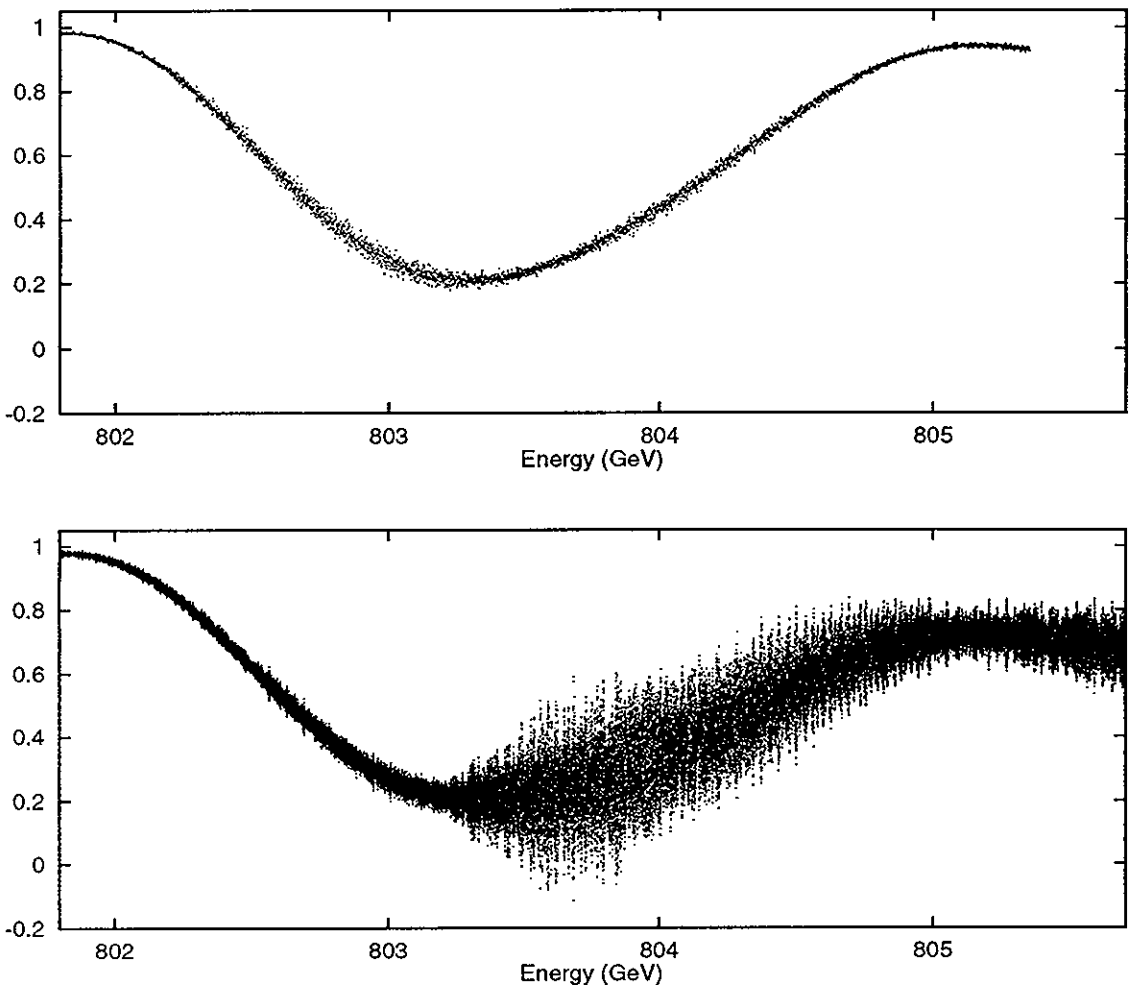

Figure 16: Behaviour of the spin motion during acceleration in HERA-p with 4 FS and 4 snakes (rrlr) and without vertical bends in the East section. Real acceleration rate. The view point is the East IP ($\langle \vec{s} \cdot \vec{n}_0 \rangle$). Top: the variant "$xyz$". Bottom: the initial transverse coordinates are the same as on the top picture but the longitudinal emittance was increased.

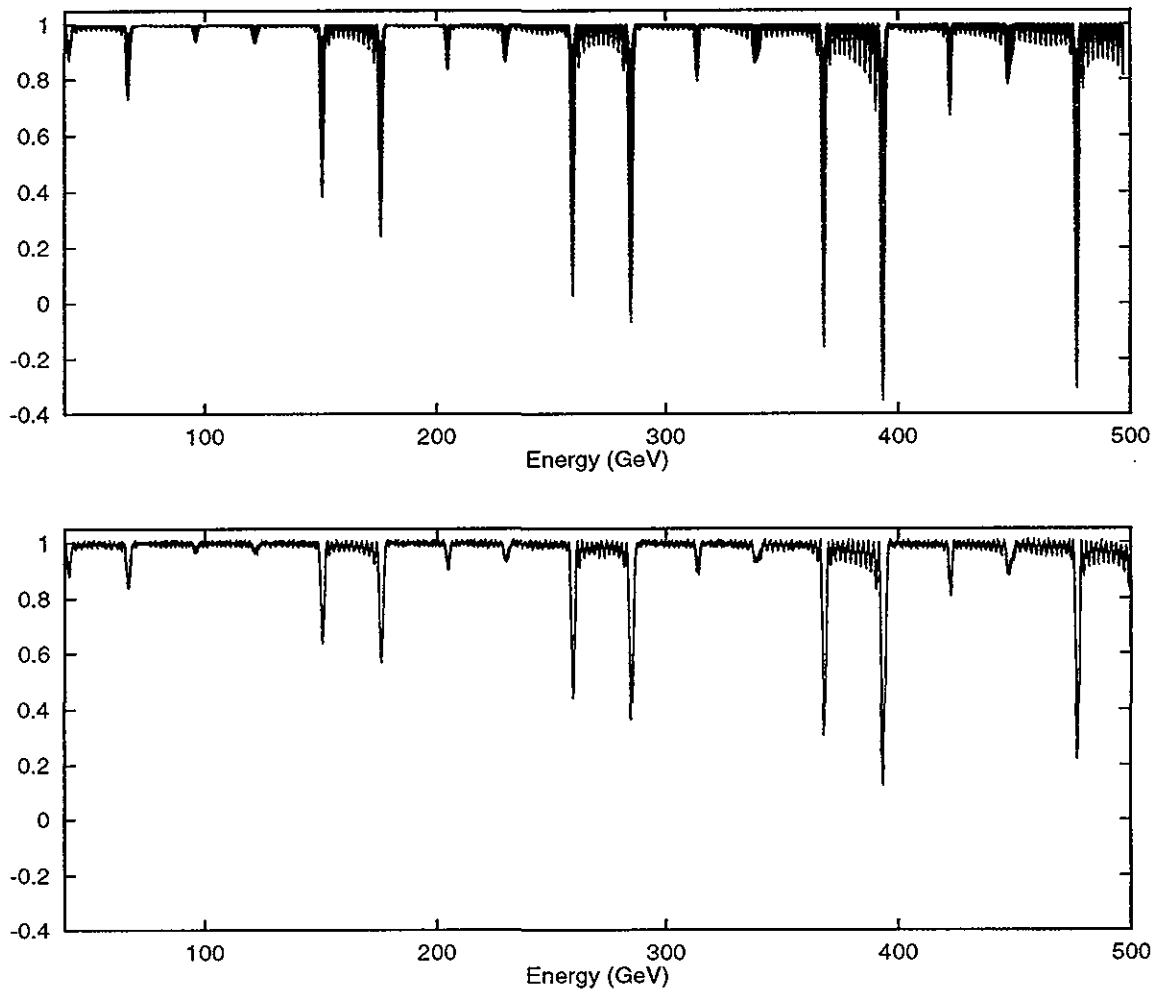

Figure 17: Behaviour of the spin motion during acceleration in HERA-p with 4 FS and 4 snakes (rrlr) and without vertical bends in the East section. The view point is the East IP ($\langle \vec{s} \cdot \vec{n}_0 \rangle$). The variant "$0y0$". Top: real acceleration rate. Bottom: increased acceleration rate (4 MeV/turn).

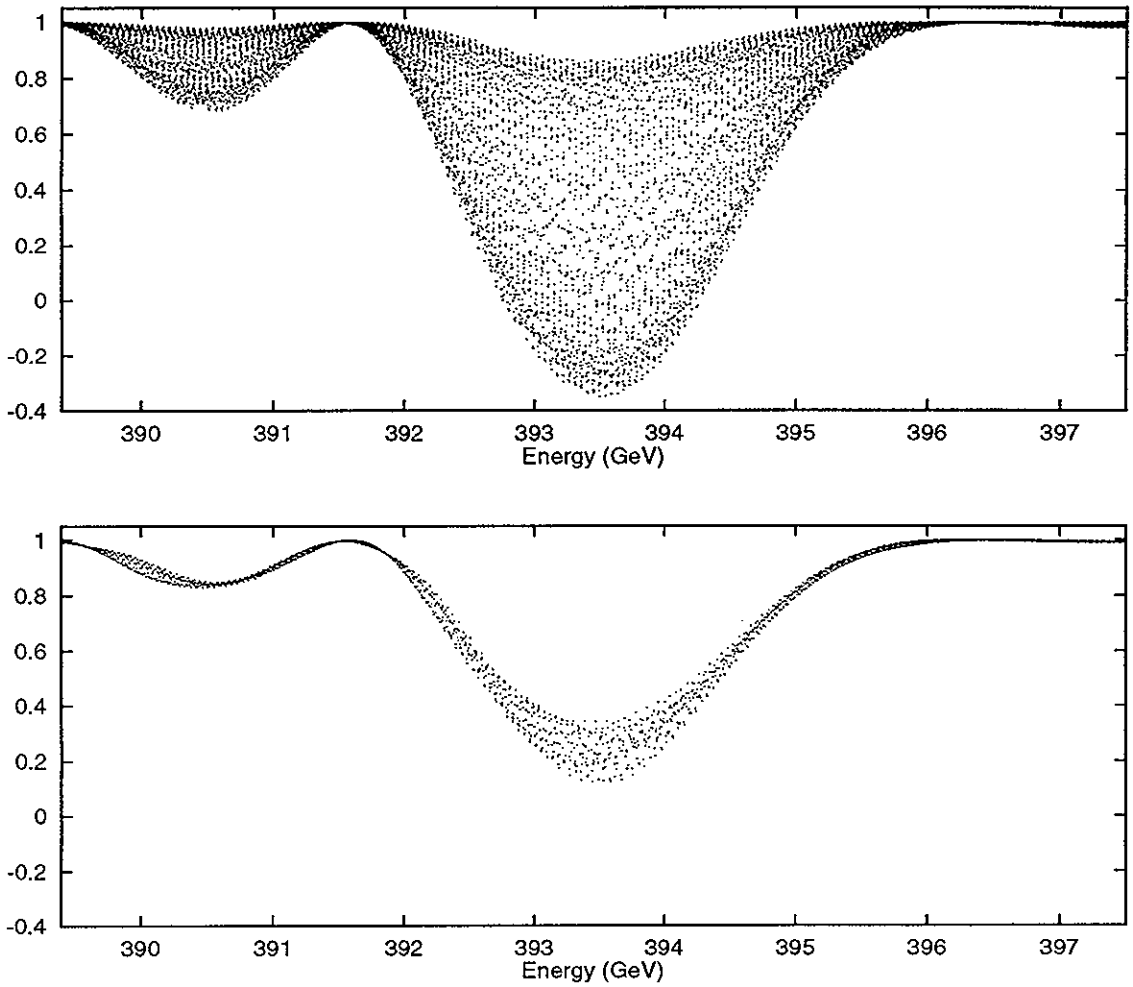

Figure 18: Behaviour of the spin motion during acceleration in HERA-p with 4 FS and 4 snakes (rrlr) and without vertical bends in the East section. The view point is the East IP ($\langle \vec{s} \cdot \vec{n}_0 \rangle$). The variant "$0y0$". Top: real acceleration rate. Bottom: increased acceleration rate (4 MeV/turn).

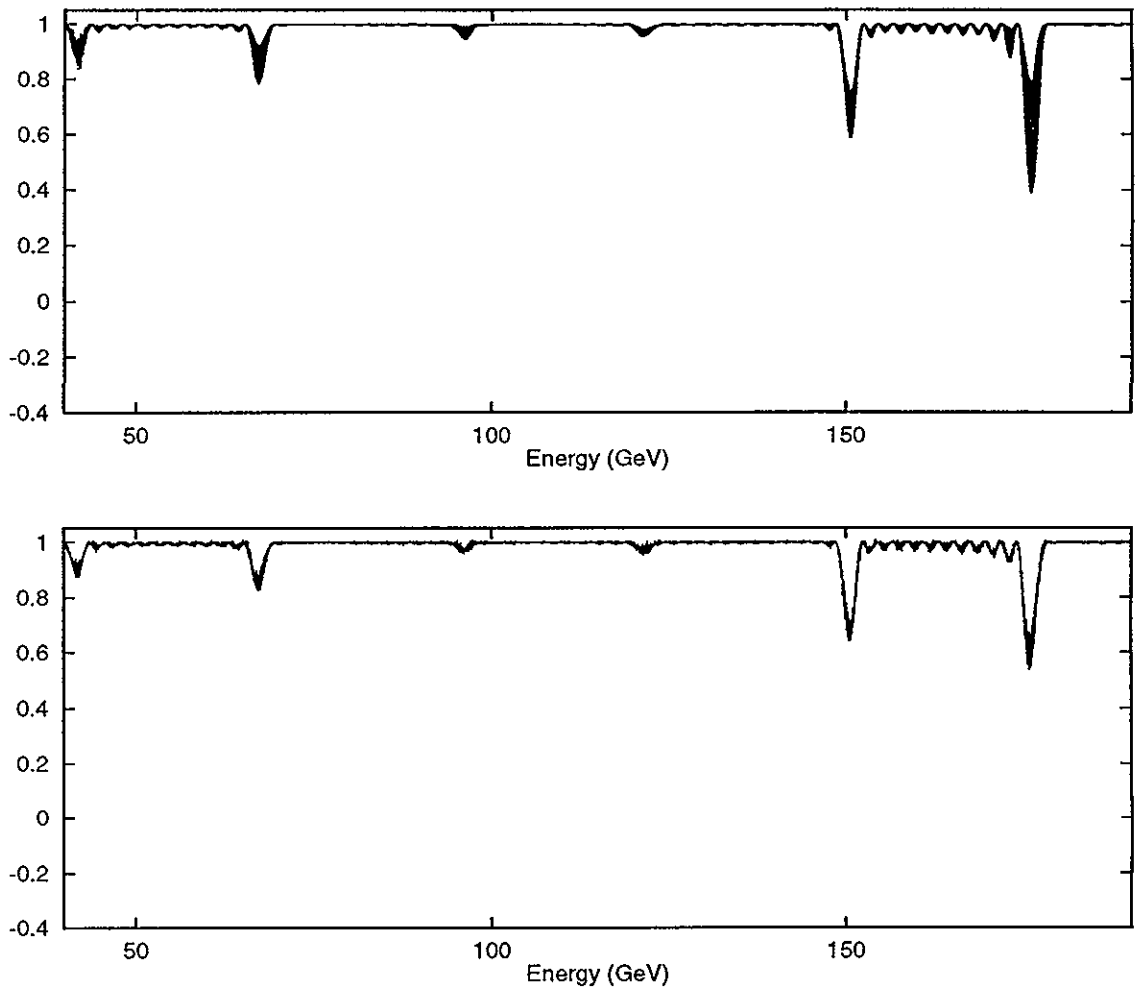

Figure 19: Behaviour of the spin motion during acceleration in HERA-p with 4 FS and 4 snakes (rrlr) and without vertical bends in the East section. The view point is the East IP ($\langle \vec{s} \cdot \vec{n}_0 \rangle$). The variant $"xy0"$. Top: real acceleration rate. Bottom: increased acceleration rate (4 MeV/turn).

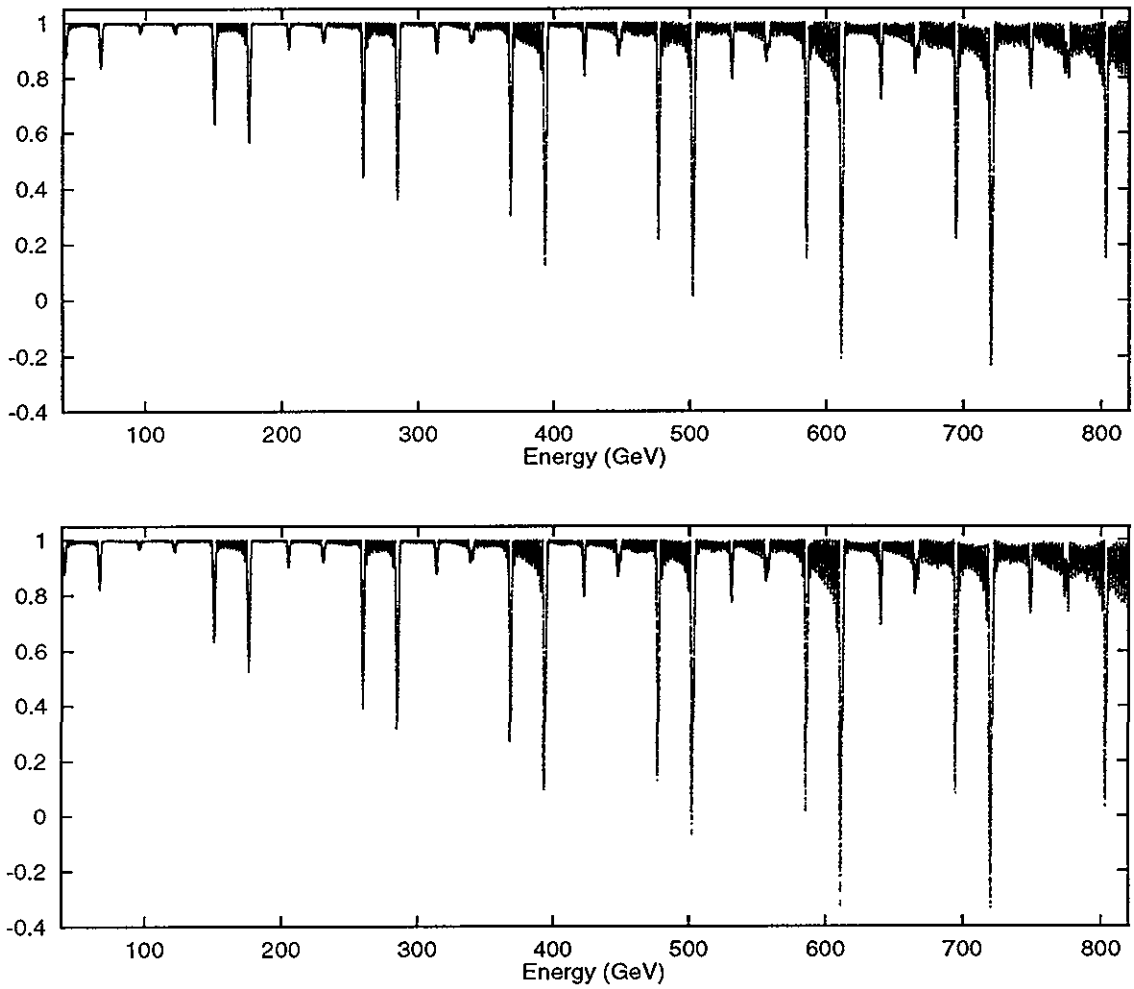

Figure 20: Behaviour of the spin motion during acceleration in HERA-p with 4 FS and 4 snakes (rrlr) and without vertical bends in the East section. Increased acceleration rate (4 MeV/turn). The view point is the East IP ($\langle \vec{s} \cdot \vec{n}_0 \rangle$). Top: the variant "$0y0$". Bottom: the variant "$xy0$".

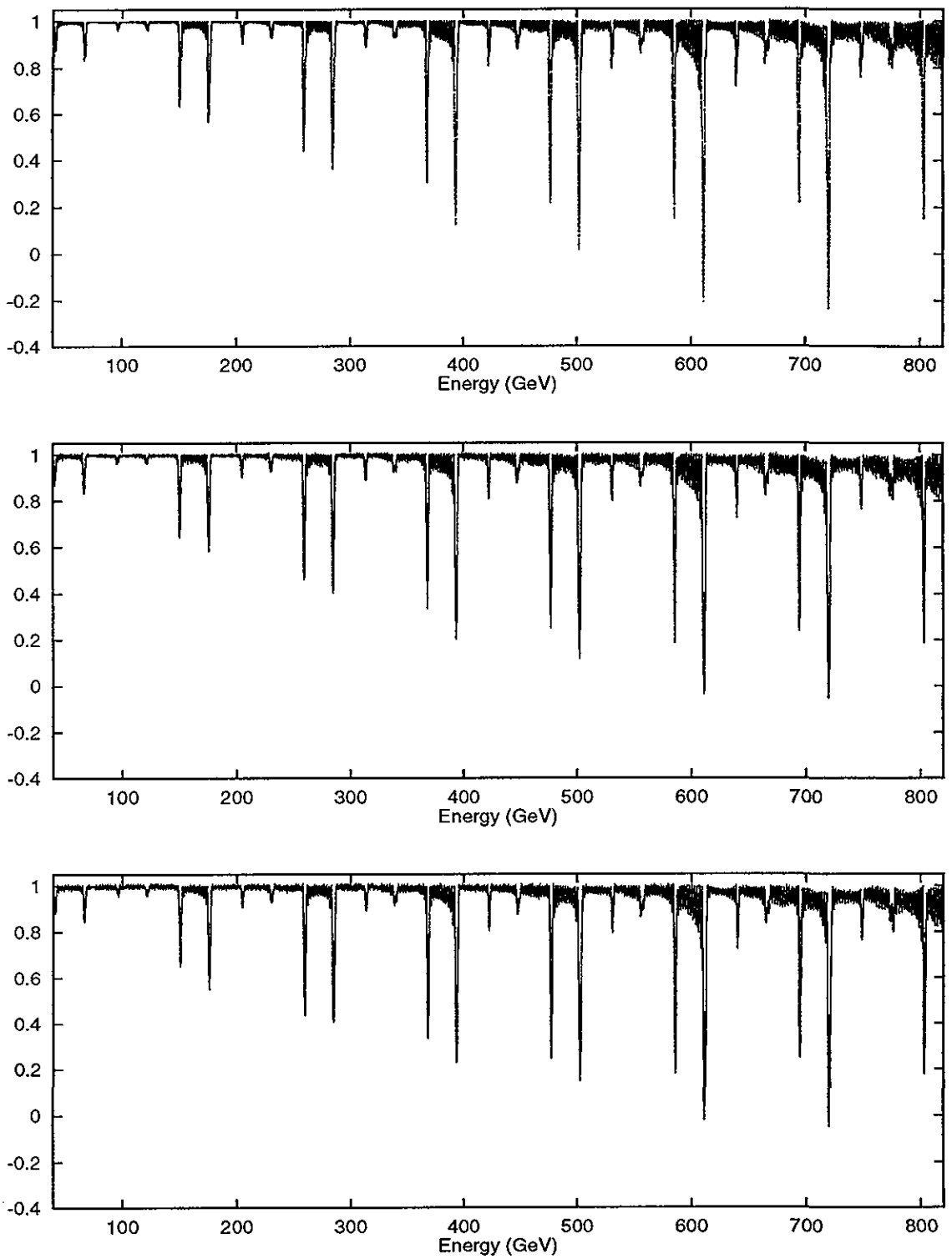

Figure 21: Behaviour of the spin motion during acceleration in HERA-p with 4 FS and 4 snakes (rrlr) and without vertical bends in the East section. Increased acceleration rate (4 MeV/turn). The view point is the East IP ($\langle \vec{s} \cdot \vec{n}_0 \rangle$). The variant "0$y$0". The number of particles: N = 4 (top), 16 (middle), 64 (bottom).

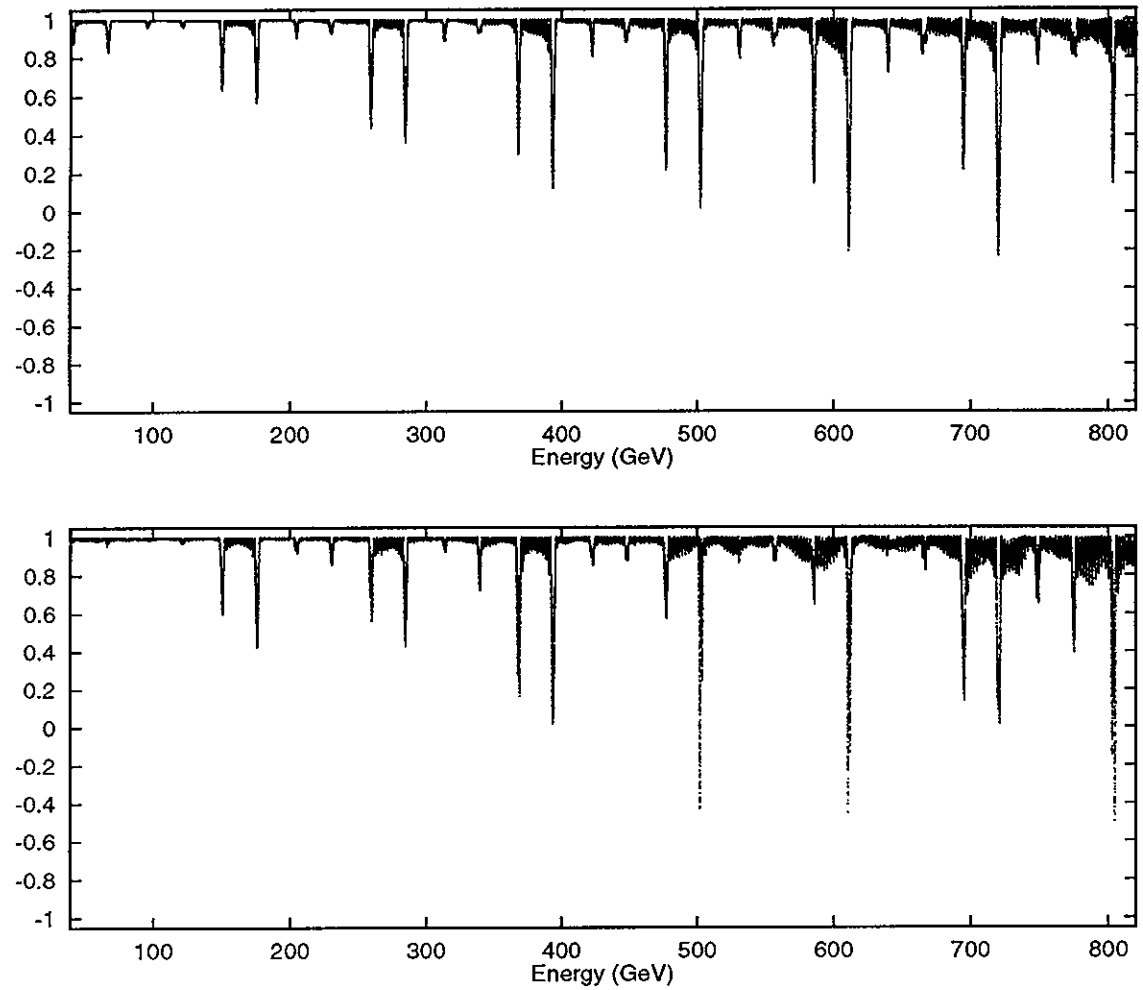

Figure 22: Behaviour of the spin motion during acceleration in HERA-p without vertical bends in the East section. Increased acceleration rate (4 MeV/turn). The view point is the East IP ($\langle \vec{s} \cdot \vec{n}_0 \rangle$). The variant "$0y0$". Top: with 4 FS and 4 snakes (rrlr). Bottom: with 4 snakes (rrlr).

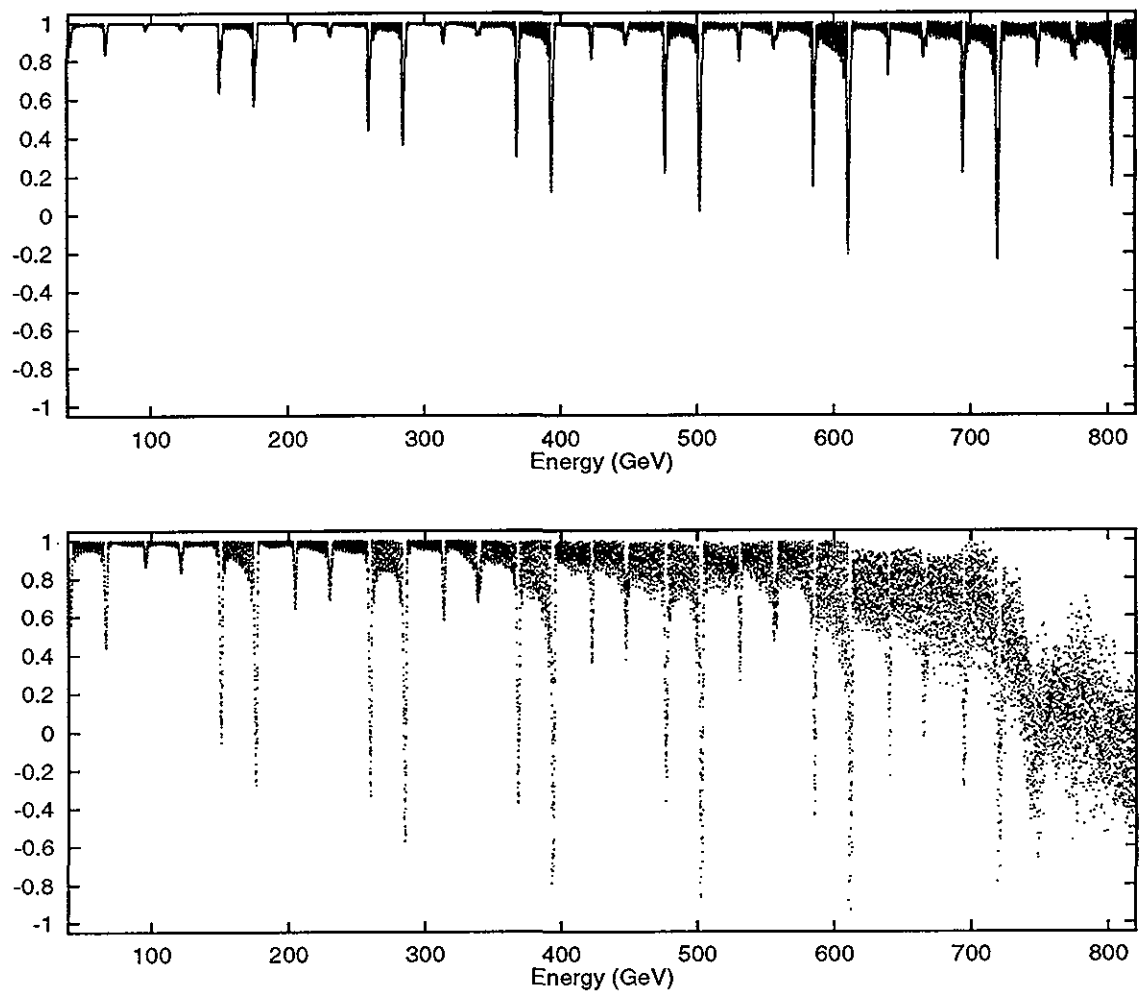

Figure 23: Behaviour of the spin motion during acceleration in HERA-p with 4 FS and 4 snakes (rrlr) and without vertical bends in the East section. Increased acceleration rate (4 MeV/turn). The view point is the East IP ($\langle \vec{s} \cdot \vec{n}_0 \rangle$). Top: the variant "$0y0$". Bottom: the variant "$0Y0$".

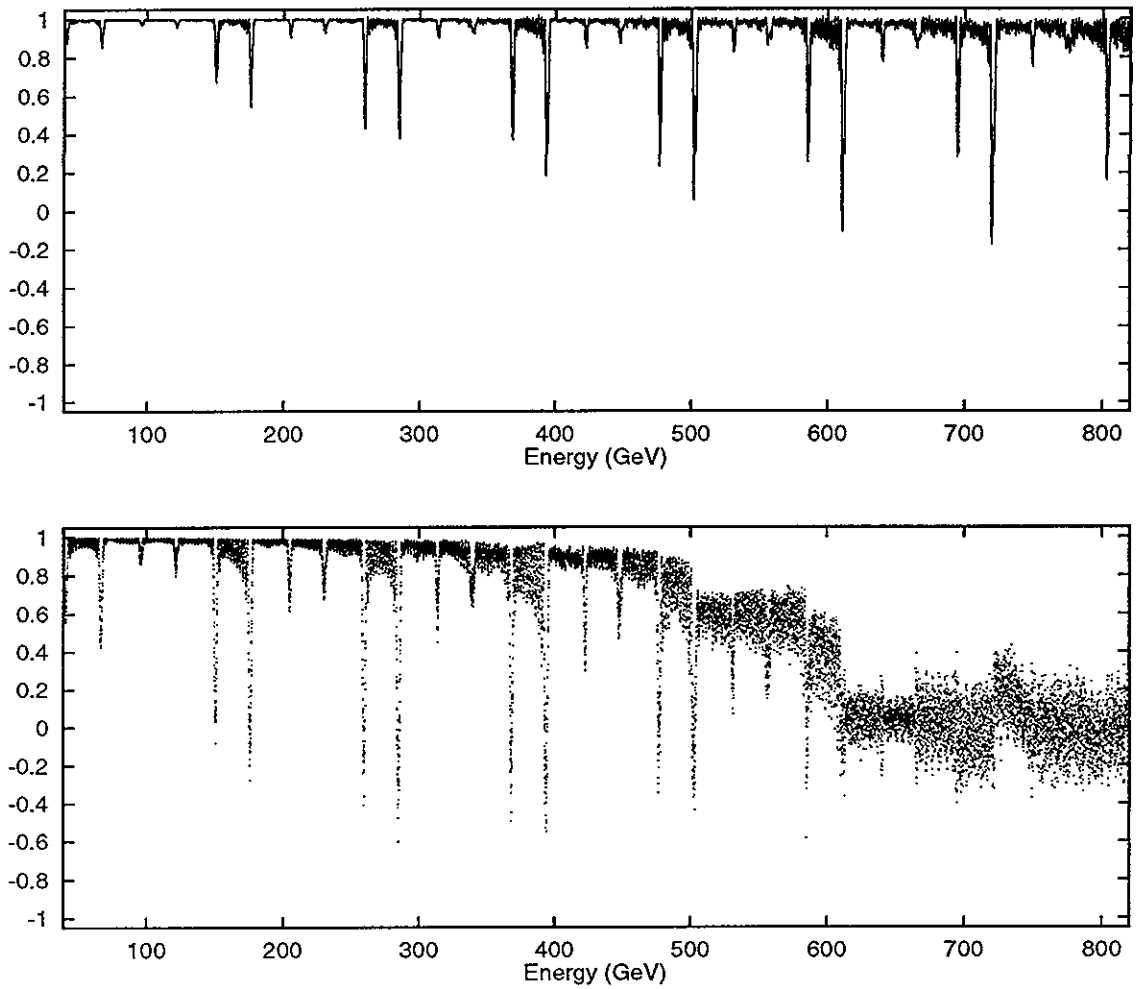

Figure 24: Behaviour of the spin motion during acceleration in HERA-p with 4 FS and 4 snakes (rrlr) and without vertical bends in the East section. Increased acceleration rate (4 MeV/turn). The view point is the East IP ($\langle \vec{s} \cdot \vec{n}_0 \rangle$). Top: the variant "$xy0$". Bottom: the variant "$XY0$".

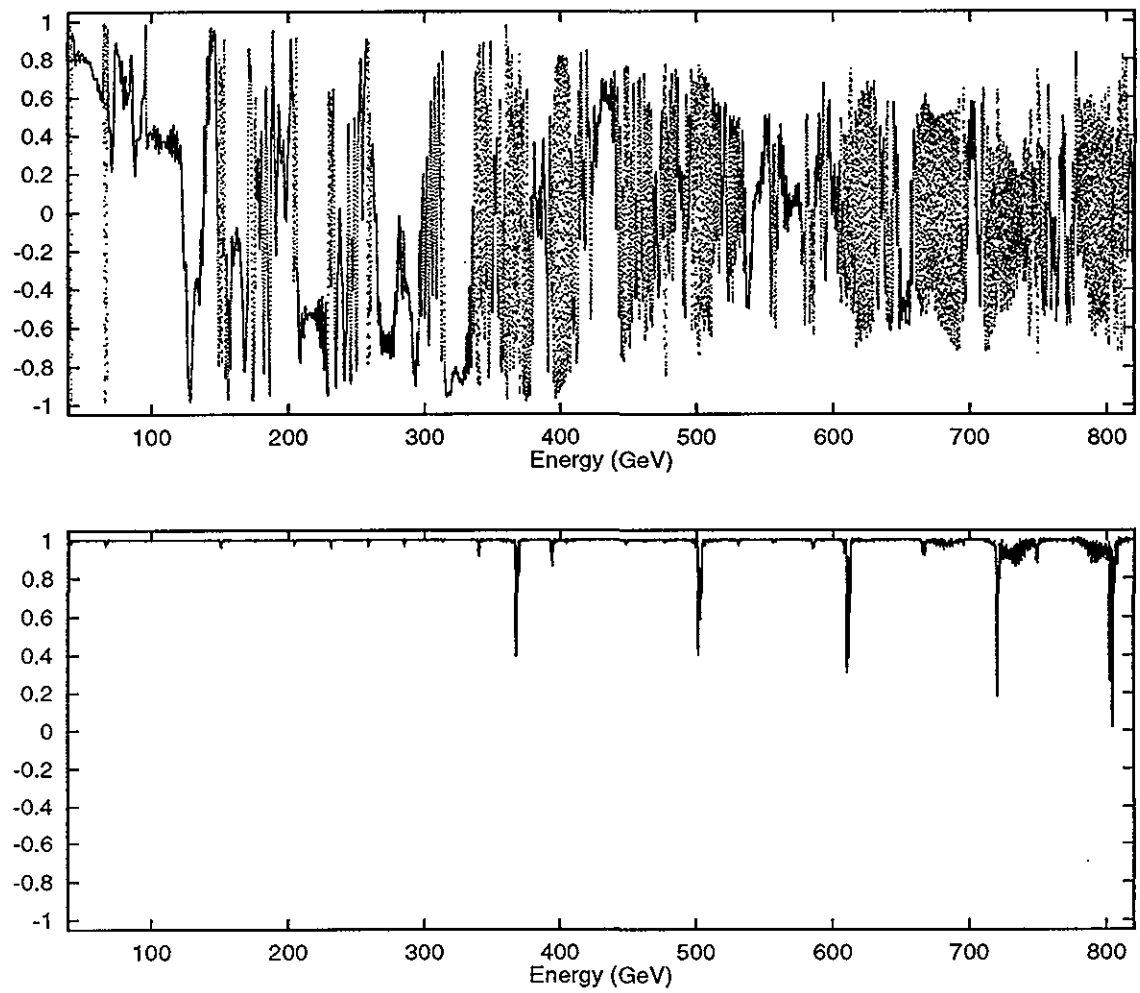

Figure 25: 4-turn spin matching for HERA-p without vertical bends in the East section. Upper: 4 snakes (rrlr) in the ring. Bottom: 4 snakes (rrlr) in the ring and one additional snake to make $\nu_{spin} = 0.17$. The view point is the East IP ($\langle \vec{s} \cdot \vec{n}_0 \rangle$). The variant "$0y0$".

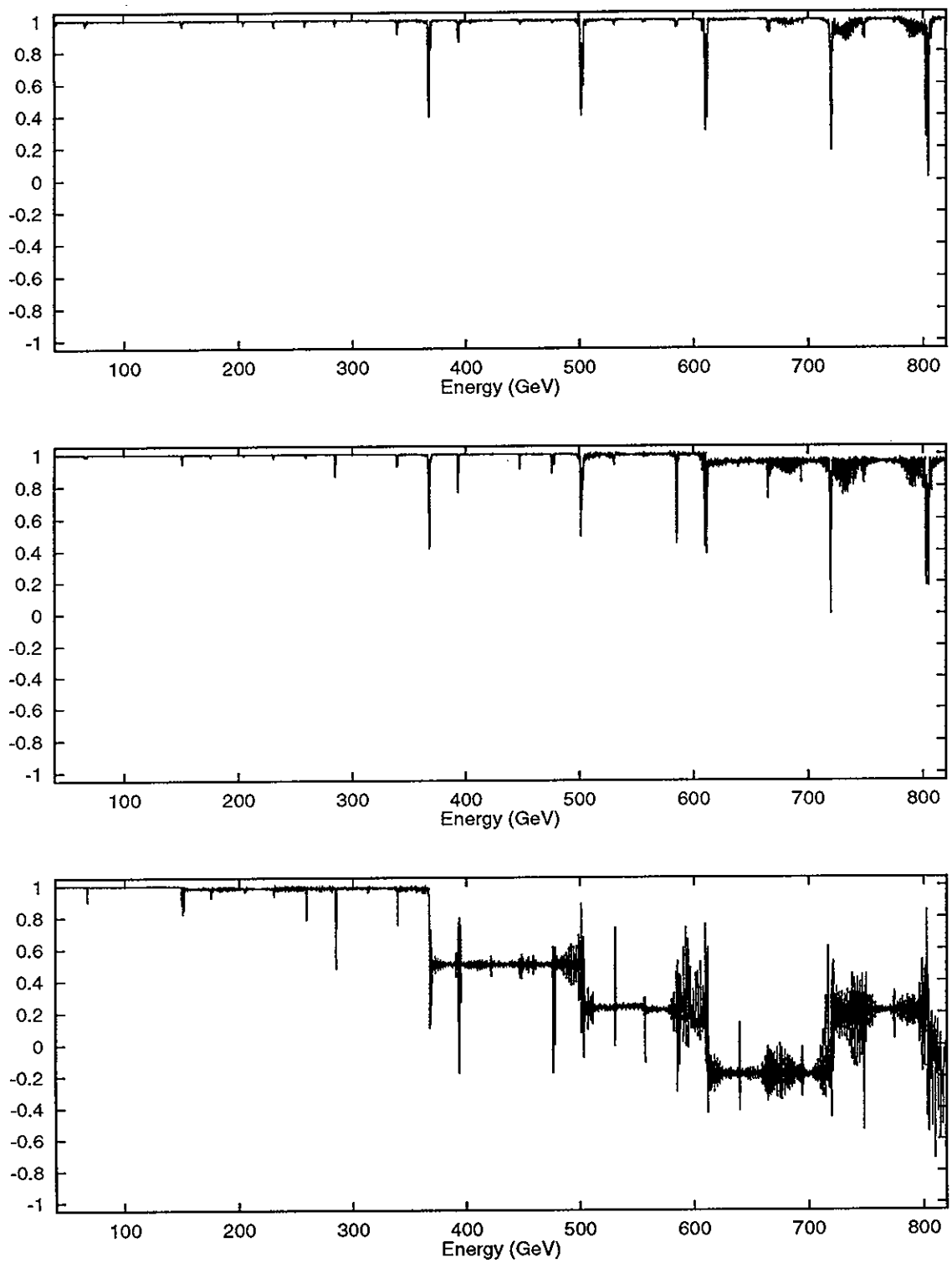

Figure 26: 4-turn spin matching for HERA-p without vertical bends in the East section. Upper: 4 snakes (rrlr) in the ring. Middle: 2 snakes (rl). Bottom: 1 longitudinal snake. The view point is the East IP ($\langle \vec{s} \cdot \vec{n}_0 \rangle$). The variant "$0y0$".

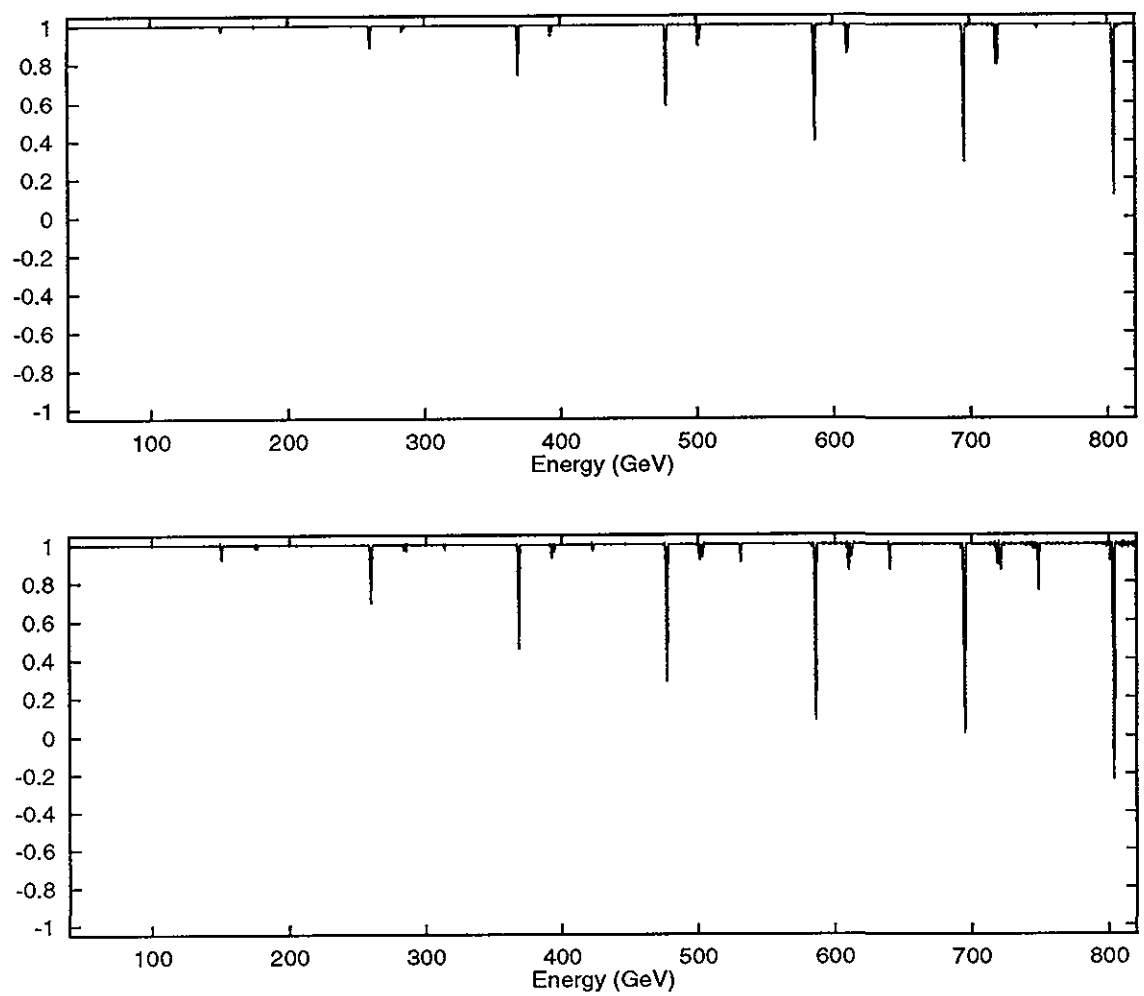

Figure 27: 1-turn spin matching for the test flat model of HERA-p. Upper: 4 radial snakes in the ring. Bottom: 4 longitudinal snakes in the ring. The view point is the beginning of the East section. ($\langle \vec{s} \cdot \vec{n}_0 \rangle$). The variant "$0y0$".

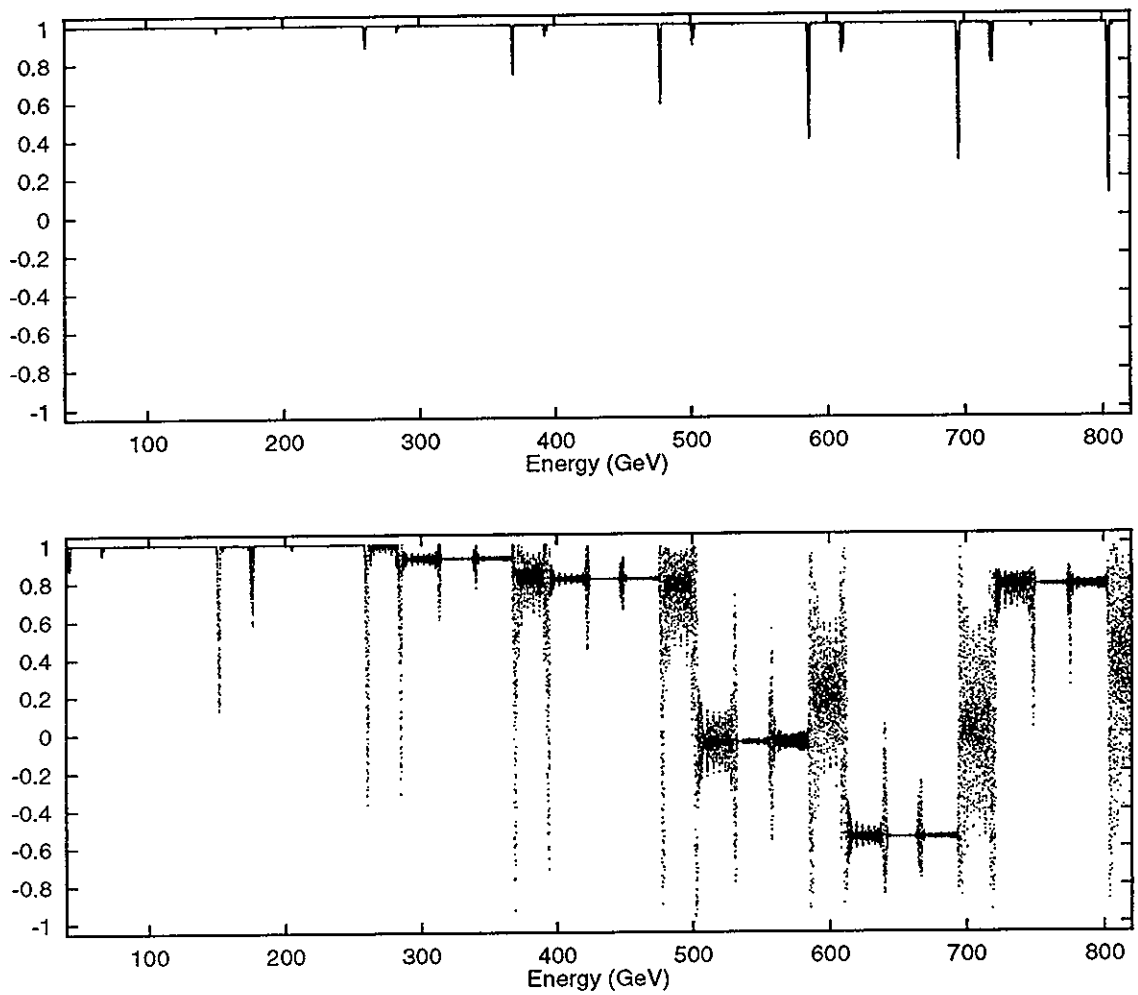

Figure 28: 1-turn spin matching for the test flat model of HERA-p with 4 radial snakes in the ring. The view point is the beginning of the East section. ($\langle \vec{s} \cdot \vec{n}_0 \rangle$). Top: the variant "$0y0$". Bottom: the variant "$0Y0$".

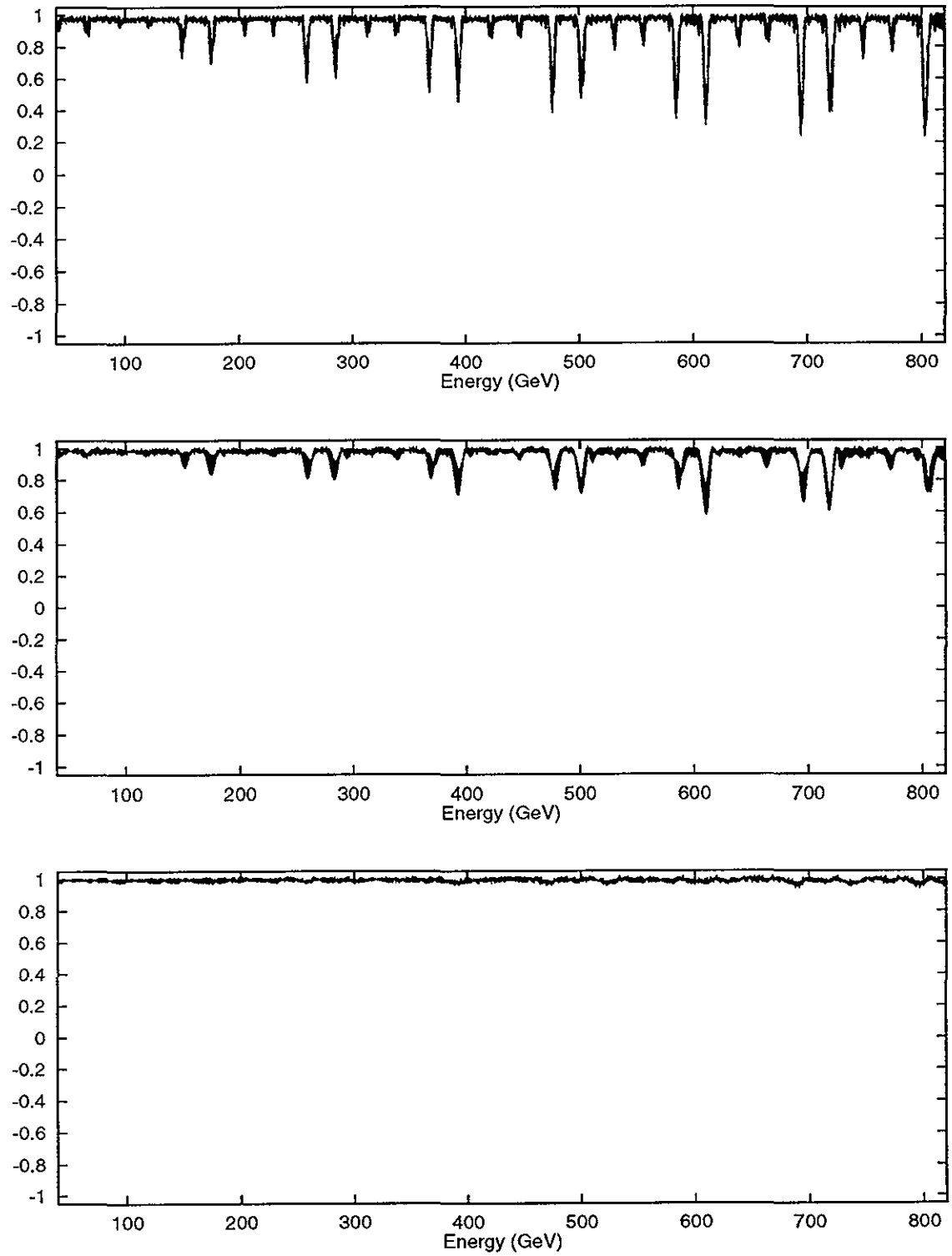

Figure 29: Behaviour of the spin motion during acceleration in the test flat model of HERA-p. Increased acceleration rate (4 MeV/turn). The view point is the East IP ($\langle \vec{s} \cdot \vec{n}_0 \rangle$). The variant $''0y0''$. Top: 8 snakes. Middle: 16 snakes. Bottom: 24 snakes.

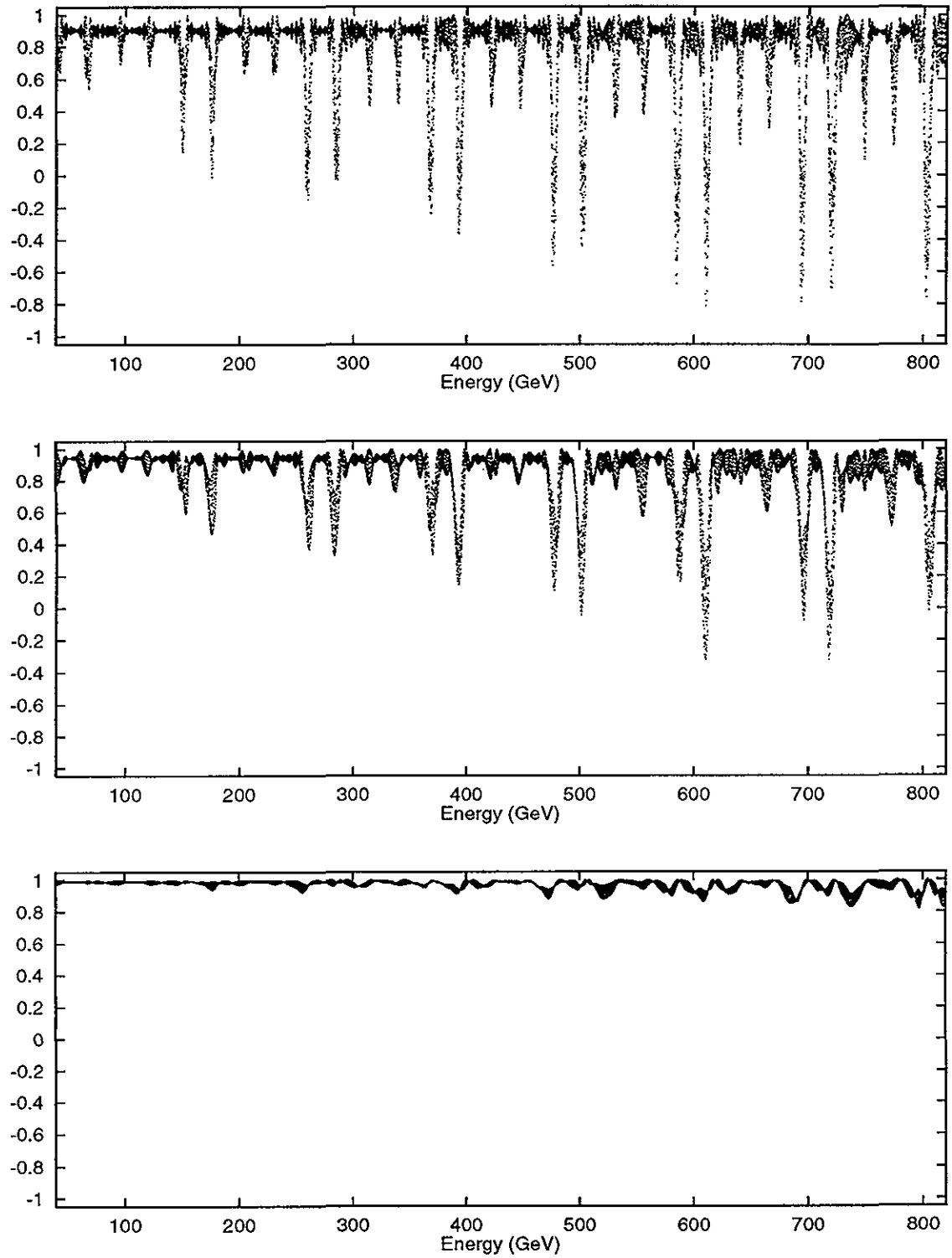

Figure 30: Behaviour of the spin motion during acceleration in the test flat model of HERA-p. Increased acceleration rate (4 MeV/turn). The view point is the East IP ($\langle \vec{s} \cdot \vec{n}_0 \rangle$). The variant "0Y0". Top: 8 snakes. Middle: 16 snakes. Bottom: 24 snakes.